ANNUAL PROGRAM REVIEW

HIGH-YIELD PULPING

March 24, 1997

ANNUAL PROGRAM REVIEW

HIGH-YIELD PULPING

March 24, 1997

Institute of Paper Science and Technology
500 10th Street, N.W.
Atlanta, Georgia 30318
(404) 894-5700
(404) 894-4778 FAX

HIGH-YIELD PULPING ANNUAL RESEARCH REVIEW AGENDA

Monday, March 24, 1997

High-Yield Pulping Annual Program Review (Room 177)

7:45 AM	Coffee and Donuts	
8:00	Welcome, Introduction, and Antitrust Statement	G. Baum S. Eachus
8:15	F012 - Southern Pine Mechanical Pulping	A. Rudie J. Kloth
9:00	F014 - Fundamentals of Brightness Reversion	A. Ragauskas
9:45	Thermal Imaging of Fiber Aggregates Subjected to Cyclic Compression	C. Rueckert
10:15	End of Morning Session	

High-Yield Pulping PAC Meeting (Room 177)

10:45	Strategic Plan and Research Lines	E. Malcolm
11:15	F014 - Fundamentals of Brightness Reversion	A. Ragauskas
12:00 PM	Lunch	
1:00	F012 - Southern Pine Mechanical Pulping	A. Rudie
1:45	RAC Report	
2:15	Meeting Closure	S. Eachus
2:30	Meeting Adjourns	

TABLE OF CONTENTS

HIGH-YIELD PULPING
PROJECT ADVISORY COMMITTEE

IPST Liaison: Dr. Alan Rudie (404) 894-9706; FAX (404) 894-4778

Mr. Richard Ain *(1998)
Research Engineer
Specialty Minerals Inc.
9 Highland Avenue
Bethlehem, PA 18017
(610) 861-3431
(610) 861-3412 FAX

Dr. Spencer W. Eachus *(1999) (Chairman)
R&D Section Leader
Union Camp Corporation
Post Office Box 3301
Princeton, NJ 08543-3301
(609) 896-1200
(609) 844-7323 FAX

Dr. Bill Frazier *(1996) (Vice Chairman)
Research Specialist
Boise Cascade Corporation
4435 N. Channel Avenue
Portland, OR 97217-7652
(503) 286-7408
(503) 286-7467 FAX

Mr. B. Robert Harley *(1999)
Director, Process/Environmental Service
Bowater Incorporated
Pulp and Paper Group - 55 East Camperdown Way
Post Office Box 1028
Greenville, SC 29602-1028
(803) 282-9372
(803) 282-9570 FAX

Mr. E. Ralph Norris *(1998)
Research Associate
James River Corporation
Camas Technical Center
349 NW 7th Avenue
Camas, WA 98607
(360) 834-8284
(360) 834-8382 FAX

Mr. David H. Robinson *(1998)
Technical Director
Champion International Corporation
West Nyack Road
West Nyack, NY 10994-0000
(914) 578-7173
(914) 578-7175 FAX

Dr. James K. Turnbull *(1999)
Section Head, High Yield Fibers
MacMillan Bloedel Inc.
4225 Kincaid Street
Burnaby, BC, CANADA V5G 4P5
(604) 439-8617
(604) 439-1254 FAX

Dr. Michael A. Veal *(1995)
Wood Fiber Scientist
Weyerhaeuser Company
WTC 2B22
Tacoma, WA 98477-0001
(206) 924-6122
(206) 924-6324 FAX

* The dates in ( ) indicate the final year of the appointment.

Southern Pine Mechanical Pulping

PROJECT SUMMARY

PROJECT TITLE: Southern Pine Mechanical Pulping

PROJECT STAFF: Alan Rudie
Alex Shaket

FY 97 BUDGET: $190,000

DIVISION: Chemical and Biological Sciences

PROJECT NUMBER: F012

OBJECTIVE: Improve the understanding of the performance limitations inherent in mechanical and chemimechanical pulping. The emphasis is on problem softwoods such as the southern yellow pines.

GOAL: Evaluate the breakdown of southern pines and spruce in the early stages of refining using a first order comminution model.

SUMMARY: Refining experiments were carried out in June of 1995 on slow growing, average density and plantation grown low density loblolly pines as well as natural stand average density spruce. The logs were debarked, chipped and refined at the Andritz Sprout-Bauer Pilot Plant using a pressurized 36-1B refiner. Three sets of identical refiner plates were obtained for the trial. One set was used as manufactured. The second set had the fine bar section removed, and the third set had the fine bar section and 1/2 of the intermediate bar section removed. Primary pulps from the full plates and intermediate section plates were also second stage refined in a Bauer 401 atmospheric refiners.

Samples from the Bauer McNett fractions were delignified with sodium chlorite and the fiber lengths determined with the Kajaani FS-100. The chlorite fibers were also analyzed by light microscopy to determine the relative percent of earlywood, latewood and transition fibers in each fraction, and the percent of each category that are whole, broken on one end and broken on two ends. This effort has been completed and shows surprisingly short average fiber lengths in TMP samples that received as little as 300 kWh/ODMT of refining energy.

An analysis of pulp bond strength was carried out using a method proposed by Sinkey in 1984. This indicates the bond strength of the low density pine is lower than the bond strength of the average density pine, at the same level of unbonded area. Evaluation of the freeness/scattering relationship suggests this low bond strength is due to a lower relative bonded area.

FUTURE DIRECTIONS:

Evidence from the existing project suggests that TMP from low density southern pines have a lower relative bonded area than TMP from average density southern pines. Among other possibilities, this can be due to a change in the distribution of lignin on/in the fibers after refining. Current project plans are to evaluate the surface composition of low and average density southern pine TMP, and the fiber lignin distribution in wood of low density and average density southern pines. Similar experiments will be conducted on spruce to serve as a reference.

PROJECT TITLE: Southern Pine Mechanical Pulping PROJECT NUMBER: F012

PROJECT STAFF: Alan Rudie
Alex Shaket

Introduction:

Wood is not a uniform material and differences in fibril angle and cell wall thickness[1] both influence the strength of fibers.[2,3] Previous research has shown that in subjecting loblolly pine to cyclic compression (simulating a disk refiner) nearly all the compressive strain and viscoelastic energy absorption occurs in the earlywood portion of the annual growth ring (Figure 1).[4] This result was largely anticipated since the elastic modulus of the earlywood (in tension parallel to the grain) is known to be about one third to one quarter of the modulus of the latewood.[5,6,7] The results suggest that earlywood is much more intensively stressed under the refining conditions than is the latewood. The implication of this is that the earlywood portion of the annual growth increment will disintegrate faster and suffer more fiber damage in mechanical pulping processes. This has been confirmed by analyzing chlorite holopulped fibers from the various particle sizes produced after very low energy pressurized refining.[8] In this research, the smaller particles, those retained on the 20 and 100 mesh screens, had a lower fiber coarseness and more earlywood fibers than the fibers in the particles retained on the 4 and 8 mesh screens (Table 1). In addition, the smaller particle size fractions contained fewer whole fibers and there was a lower percentage of whole earlywood fibers than whole latewood fibers in all the size fractions (Table 1).

Table 1 Fiber coarseness and fiber length of various particle size fractions after low energy refining.

Mesh Size	Coarseness mg/M	Fiber Length mm	% Whole Fiber	
			EW	LW
4	0.22	3.21	37	59
8	0.21	2.41	18	35
20	0.17	2.62	1	23
100	0.18	1.21	0	3
EW	0.16	2.80		
LW	0.38	3.26		

The uneven energy absorption in the early stages of disk refining fragments the earlywood fibers. This makes them less able to contribute to the strength of the product and results in both wasted energy and a weaker paper. Because Douglas fir and the southern yellow pines contain large amounts of latewood, and the difference between the specific gravity, elastic modulus and tensile strength of the earlywood and latewood is very large,[5,6,7] these species suffer acutely from the concentration of refining energy in the earlywood and produce low strength mechanical pulps.[9,10]

This task was established to continue the evaluation of wood breakdown into fiber during disk refining. Using the methods established earlier,[8] the project followed the breakdown of wood and the liberation of fibers through the specific energy range of 200 to 2,000 kWh/odmt.

SUMMARY OF PRIOR WORK

Wood Characterization:

Wood parameters are summarized below. All wood is under 15 cm (6") diameter since this was the limitation of the IPST chipper. On average, the final growth ring of the fast growth pine was the only one with a high level of latewood, indicative of mature wood character. The slow growth pine typically had 7 to 10 years of high latewood content, growth rings. The fast growth pine was low density at 0.41 g/cc and the slow growth pine was slightly above average for loblolly pine at 0.49 g/cc. The spruce, at 0.43 g/cc, was also a little above average density.

Table 2: Wood Characterization

Wood	Sp. Grav.	Latewood	Ring Width	Age
Spruce	0.43		1.3 mm	46
Slow Pine	0.49	40.4%	4.2	13.8
Fast Pine	0.41	30.2%	9.1	6.2

Refining Pilot Trial

The wood was debarked, chipped and refined at ASB on June 8, 9 and 16, 1995. Samples were prepared using full size refiner plates (D14B001), similar plates with the fine bar section removed, and plates with both the fine bar and 1/2 of the intermediate sections removed. Primary refining was carried out in a Sprout type 36-1CP pressurized refiner operating at 2,000 rpm. Primary pulps from the full plates and intermediate section plates were second stage refined in a Bauer 401 atmospheric refiner.

Fully refined pulp properties were as expected with the exception that the spruce was very dry and the refining conditions were not adjusted appropriately when using the whole plates. This pulp sample is very poor with a maximum tear index of 3.1 $mN \cdot m^2/g$ and tensile index of 25.3 N·m/g. A typical spruce pulp from the Andritz Sprout Bauer Pilot Plant gives a maximum tear index around 10 $mN \cdot m^2/g$ and a tensile index of 40 to 50 N·m/g. This data is not used in the analysis. The spruce sample obtained using the refiner plates with the fine bar section removed gave a much better quality pulp. This gave the strongest pulp obtained in this project, with a tear index of 8.9 $mN \cdot m^2/g$ and tensile index of 32.1 N·m/g at 1.8 MWh/ODT specific refining energy. The slow growth rate pine gave a tear index of 5.6 $mN \cdot m^2/g$ with 18.9 m·N/g tensile index at 2.0 MWh/ODT and the fast growth rate pine gave a tear index of 4.9 $mN \cdot m^2/g$ and tensile index of 16.3 N·m/g at a specific refining energy of 2 MWh/ODT. On pine, the refiner plates without the fine bar section

gave much poorer pulp quality than the whole plates.

Using the full refiner plates, the first stage refiner specific energy applications ranged from 700 kWh/ODT for the spruce to 1,000 kWh/ODMT for the loblolly pines. These samples contained 10 to 17% Pulmac 0.010" shives and 15 to 30% fines. Specific energy consumption ranged from 300 to 400 kWh/ODT on pine and 700 kWh/ODT on spruce when using the plates with the intermediate bar section removed. These pulps contained 20 to 50% shives and 15 to 20% fines. Using the smallest set of plates, with the fine bar section and half of the intermediate bar section removed, specific energies ranged from 200 to 300 kWh/ODT for all three wood sources and the resulting pulps all contained greater than 40% shives and less than 15% fines.

Comminution Theory

Particle comminution theories have been used to describe wood disintegration in refining before.[11,12,13] The analysis in this research has been carried out using a strictly first order approach and has been carried out in three ways: a single rate process for the reduction in the R_{14} mesh fraction, a single rate process for the reduction in Pulmac 0.01" shives, and a detailed six rate process evaluating the rate of reduction and formation of the R_{14}, R_{28}, R_{48}, and P_{48} mesh fractions.

If k is the first order rate of disappearance of the R_{14} mesh fraction, k_1 is the first order rate at which R_{14} forms R_{28}, k_2 is the rate at which R_{14} forms R_{48}, and k_3 is the first order rate at which R_{14} forms the pass 48 mesh (P_{48}) fractions, the parallel process abides by the following equality

$$k = k_1 + k_2 + k_3$$

The other disintegration rates contributing to the fragmentation process are: k_4, the rate at which R_{28} breaks down into R_{48}, and k_5, the rate at which R_{48} breaks down to form P_{48}. The process $R_{28} \rightarrow P_{48}$ has not been considered since this would be difficult to distinguish from k_4 and k_5.

Comminution rate analysis, R_{14}:

The resulting constants for R_{14} reduction and shive reduction are given in the following table, along with the r^2 for the regression analysis. Also summarized in the following table is the initial rate of reduction in R_{14} estimated in the four fraction analysis. In this case, the initial constant is adjusted to match the rate of formation of R_{28}, R_{48} and P_{48}. For this reason, results differ slightly, but in most cases insignificantly from the single rate procedure. In general, the three methods of analysis give similar results. The rate of wood breakdown is in the range of 22 to 25 ODMT/kWh for all three wood species using both the full plates and the plates with the fine bar section removed. The rate of wood breakdown is significantly higher for the spruce with the whole plates, the sample refined under very dry conditions. The similarity of the initial disintegration rates for the primary refiner with all three plates, and the primary refiner with whole plates combined with the secondary refining, confirms that the disintegration mechanism has not been significantly changed by the plate modifications.

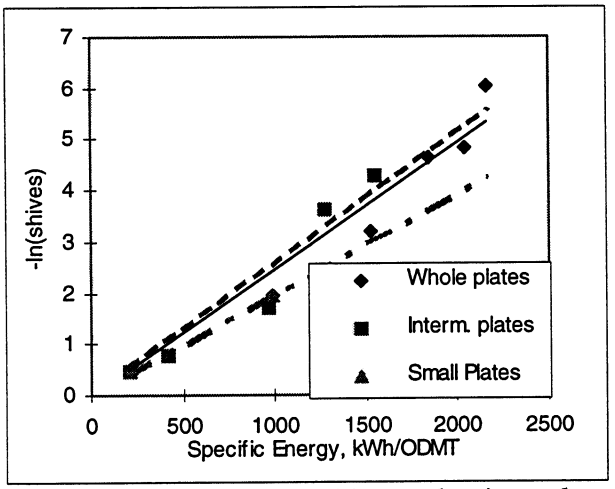

Figure 1. First order shive reduction, slow growth pine.

Extended Comminution Analysis, R14, R28, R48 and P48:

The rate equations for formation and breakdown of the four Bauer McNett fractions were solved manually by entering the equations in a spread sheet and adjusting each k iteratively. The r^2 from a linear regression analysis of the real values in each fraction against the calculated values was used as the fit parameter. The resulting comminution constants and final r^2 for each case is given in table 4. The most significant deviations from the model all occur at low energy. This may be due to difficulties in obtaining good energy measurements under these conditions, but is more likely due to the physical constraints of the initial chip breakdown in refining. Since wood chips cannot fit between the refiner plates, there is a massive amount of chip destructuring that must take place before the wood chips pass through the breaker bar section of the refiner. This physical limitation should dominate the refining mechanisms at low energy.

Table 3: First Order Wood Disintegration Rates using R14 and Shives

Wood	Plates	Four Fraction Analysis	R 14 Data k (ODMT/kWh)	r^2	Shive Data k (ODMT/kWh)	r^2
Spruce	Whole	0.0041	-0.0041	0.86	-0.0038	0.94
Spruce	Intermediate	0.0025	-0.0019	0.91	-0.0021	0.98
Spruce	Initial		-0.0037	0.61	-0.0028	0.86
Slow Pine	Whole	0.0023	-0.0017	0.89	-0.0024	0.95
Slow Pine	Intermediate	0.0025	-0.0027	0.86	-0.0026	0.92
Slow Pine	Initial		-0.0020	0.69	-0.0020	0.99
Fast Pine	Whole	0.0019	-0.0020	0.94	-0.0025	0.93
Fast Pine	Intermediate	0.0025	-0.0030	0.91	-0.0027	0.90
Fast Pine	Initial		-0.0020	0.89	-0.0023	0.72

The pattern of wood breakdown into individual fibers and fiber fragments is slightly faster using the intermediate plates. Besides higher rate constants, this also shows up as a 10 point loss in long fiber (R_{28}) and a 30% loss in tear strength in the pine samples and is consistent with an increase in refining intensity. The differences in the patterns of wood breakdown between wood sources are quite informative. The slow and fast growth pine break down at nearly identical rates, but the slow growth generates less long fiber (k_1) and more broken fiber (k_2) and P_{48} mesh (k_3) material in the initial parallel breakdown process. For the fast growth pine the rates in the series breakdown process (or secondary refining) are much faster. The value of k_4 for the fast growth rate pine is three times that of the slow growth pine, and the value of k_5 for the fast growth pine is 4 times that of the slow growth pine. The pulps produced with the intermediate plates are similar.

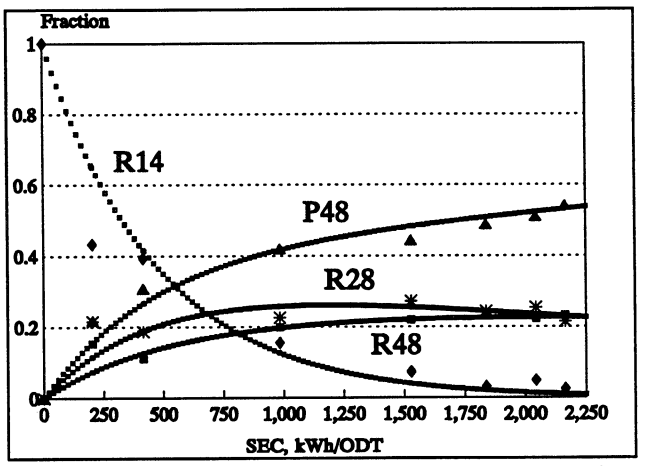

Figure 2. Slow growth southern pine comminution rates using the full plates. $R^2 = 0.9$

Table 4. Comminution rate constants, units are ODT/kWh.

	R_{14}	14->28	14->48	28->48	14->P_{48}	48->P_{48}	r^2
	k	k_1	k_2	k_4	k_3	k_5	
FP W	0.00186	0.0011	0.00035	0.00067	0.00041	0.00082	0.946
FP I	0.0025	0.0014	0.00033	0.0014	0.00077	0.0013	0.942
SP W	0.0023	0.00080	0.00046	0.00023	0.00104	0.00019	0.917
SP I	0.0025	0.00095	0.00058	0.00067	0.00097	0.00076	0.832
S W	0.0041	0.00135	0.00057	0.0025	0.00218	0.0019	0.994
S I	0.0025	0.0009	0.00065	0.0002	0.00095	0.00033	0.907

FP is fast growth pine, SP is slow growth pine, S is spruce. W is wood refined using the whole plates and I indicates the refining was carried out with the intermediate plates (the plates with the fine bar section removed).

Fast growth pine generates more long fiber in the primary refining, but it does not survive the secondary refining process and at usable freeness levels, the fast growth pine has less long fiber than slow growth material. The spruce sample prepared with the intermediate plates has very similar initial breakdown rates to the slow growth pine. On the other hand, k_4 and k_5 are about half the corresponding rates in the slow growth pine, a much slower generation of short fiber and fines. At 1500 kWh/ODT, the spruce sample has about 45% P_{48} material compared to almost 60% for the slow growth pine and 62% for the fast growth pine.

REVIEW OF 96/97 ACTIVITY:

Fiber Length Analysis

Fiber length analysis were carried out on the TMP pulps by Andritz Sprout-Bauer, using the AS-B FiberScan® instrument. The primary refiner samples were also fractionated at IPST using coarse screens. These Bauer McNett fractions, and samples of the original wood chips, were delignified using the acid chlorite process,[14] disintegrated and analyzed using the IPST Kajaani FS-100®. Both sets of fiber length analysis (Number Average) are reported in table 5. The very coarse 4 mesh and 8 mesh wood particles show some reduction in fiber lengths relative to the starting wood chip fiber length. Initial fiber length measurement on the coarse, 4 and 8 mesh fractions gave Kajaani number average fiber lengths between 1.22 mm and 0.9 mm. Because of the very short fiber lengths and concerns about the use of glass beads to disintegrate the chlorite treated particles, the disintegration step was checked by shaking kraft fibers in the glass bottles for several hours and monitoring the change in fiber length. The average fiber length from four replicate experiments decreased by 22% over three hours. Although the loss in fiber length was not statistically significant it was enough to cause concern about the method and it was decided to repeat the chlorite treatments. The disintegration had been carried out after about two chlorite treatments when some of the larger wood particles were not completely delignified. To avoid problems, this time the treatments were extended until the particles broke up with minimal agitation. In addition, the original wood chips were chlorite treated to obtain fiber length data for the starting material. The new data is reported in Table 5.

A sample average fiber length was estimated from the chlorite holopulped, Bauer McNett samples by multiplying the Kajaani number average fiber length of each fraction by the fraction weight % and summing the contribution from all fractions.[15] Note that the duplicate measurement of the samples prepared with the smallest refiner plates give similar fiber lengths even though they were analyzed using different sets of screens in the Bauer McNett. This estimated fiber length is technically a weighted average and listed as L^2 in table 5. These values are similar to the number average fiber length of the fully refined pulps listed as L, and is shorter than the number average fiber length found for the wood and also listed under L. Because of the changes in measurement instruments and methods, small differences are not very meaningful, but this data provides very strong evidence that the majority of fiber damage occurs early in the refining process, before a specific energy consumption of 200 kWh/ODT. Similar results have been reported by Heikkurinen *et al.* for 8 mesh and 14 mesh fractions from 500 kWh/ODT TMP and RMP.[16]

The first stage refiner samples after Bauer McNett fractionation and chlorite holopulping were analyzed by optical microscopy to determine earlywood/latewood ratio and the fraction of unbroken fibers. Some of this data was reported at the last Annual Review. The completed data is summarized in table 6. It was predicted that the smaller particle size fractions would be enriched in earlywood after low energy refining. Evidence for this had been observed earlier in a laboratory study[8] but this is not confirmed in this study. The data for samples prepared with the small plates and 200 to 300 kWh/ODMT specific energy is most useful for this analysis. For all three wood species, the small particle size fractions, representing single fibers and single fiber fragments, is enriched in latewood fibers, not earlywood fibers. The only sample that shows a significant

enrichment of earlywood fibers in the smaller size fraction is the fast growth rate pine sample prepared with whole refiner plates. This disagrees with the results of the earlier laboratory experiments using the Defibrator D. The contradiction could be due to a difference in refining mechanisms between the disc refiner and drum type Asplund mill, or could reflect a change in the process between the 20 kWh/t specific energy level applied in the Defibrator D, and the 200 kWh/t specific energy applied with the smallest set of plates at Andritz Sprout-Bauer.

Table 5. Fiber length measurements on TMP and chlorite delignified coarse particles.

	kWh/ ODT	L	L^2	4 mesh	8 mesh	14 mesh	28 mesh	48 mesh	100 mesh	200 mesh
Fast P	Wood	1.61*								
	250	1.46	1.23	1.46		1.35		1.26	0.69	
	250	1.46	1.33	1.66	1.44	1.26	1.38			
	319	1.43	1.06		0.90	1.14	1.53		1.18	
	921	1.68	1.24			1.16	2.23	1.35		0.40
	2223	1.27								
Slow P	Wood	1.9*								
	204	1.42	1.33	1.55		1.50		1.45	0.83	
			1.35	1.70	1.58	1.41	1.41			
	416	1.61	1.17		0.96	1.20	1.85		1.26	
	984	1.31	0.77			1.29	2.24	1.35		0.4
	2165	1.31								
Spruce	Wood	1.36*								
	204	1.38	1.12	1.26		1.31		1.06	0.66	
			1.51	1.31	1.19	1.23				
	688	1.29	1.07		1.10	1.10	1.74		0.97	
	715	0.68	0.49			1.00	1.01	0.97		0.4
	1539	1.09								
	1795	1.27								

* Wood fiber lengths are on chlorite holopulped wood chips and are analyzed using the Kajaani FS-100. All other number average fiber lengths were determined by Andritz Sprout-Bauer using the Fiberscan instrument.

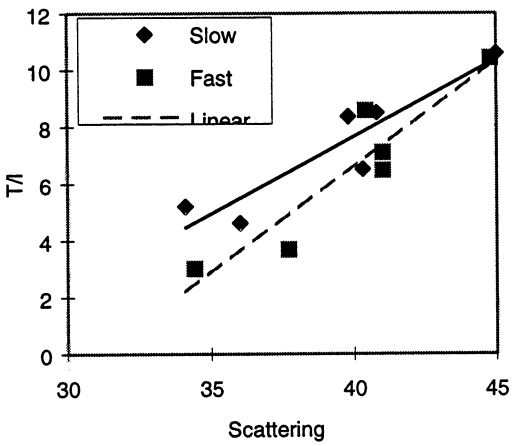

Figure 3. Sinkey bond index relative to scattering coefficient (unbonded surface area) for low and high density loblolly pine.

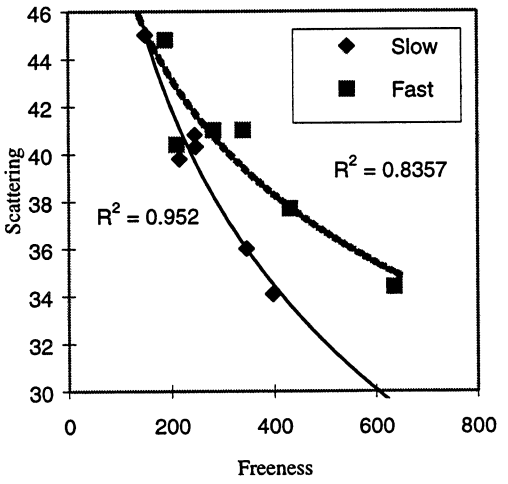

Figure 4. Scattering coefficient relative to pulp freeness in low and average density loblolly pine.

On-going laboratory work at IPST does show little or no preferential energy absorption between earlywood and latewood fibers when fiber aggregates are subjected to cyclic compression, confirming a change in refining mechanism once wood chips are rendered to fiber.[17] For the pilot plant samples, between 25 and 40% of the pulp prepared using the smallest set of plates, was retained on an 8 mesh screen. In the prior lab experiments, 65% of the material was retained on the 8 mesh screen. The difference in outcomes of the laboratory and pilot scale experiments may well be due to the large difference in specific energy consumption between the two experiments and the change in the refining mechanism of wood and fiber aggregates, observed in the laboratory.[4,16]

On average, there are about thirty percent more whole latewood fibers in all size fractions and all three refining conditions. The earlywood fibers clearly have a higher probability of being broken in refining and this result is independent of species and refining conditions

Handsheet Analysis

Handsheets were prepared and tested by the Andritz Sprout-Bauer Laboratory. In general, the pines produced low tensile and tear strength pulps relative to the spruce pulp produced with the intermediate plates. In addition, at a given specific energy, the fast growth pine produced low tensile and tear strength pulps relative to the slow growth pine. In an evaluation of tensile models of paper, Sinkey determined that the ratio of tensile index to fiber length was proportional to fiber bond strength.[18] Although this theory has never been rigorously validated, the method offers a means to evaluate the nature of bonding in these pulps. A plot of the Sinkey bond index relative to paper scattering coefficient (as a measure of unbonded surface area) is given in figure 3. A second plot of scattering coefficient (unbonded area) relative to freeness (total surface area) is shown in figure 4. The bond index gives straight line relationships with scattering, and suggests the fast growth rate pine has a lower bond strength at a given unbonded surface area than the slow growth wood. This can potentially be caused by either a decrease in relative bonded area, or a decrease in specific bond strength. The graph of scattering coefficient relative to pulp freeness shows that at a low total surface area (high freeness) the scattering coefficient of the fast growth pine is much higher than the scattering coefficient of the slower growth pine. This suggests that at a given total surface area, the unbonded surface area of the fast growth wood is much higher, and

therefore, the bonded area of the fast growth rate wood is much lower than in the slow growth pine. A similar analysis has been carried out on pilot plant data from the Georgia Tech Center For High Yield Pulp Science. The original data from this study had been reported previously at the 1991 Annual Review. This data showed the same relationships between bond index, scattering coefficient and pulp freeness as observed in figures 3 and 4. The two samples compared were a slower growth southern pine with a density measured at 0.53 g/cc, and a faster growth rate sample with a density measured around 0.46 g/cc. Both samples were of 24 year old trees, considered to be mature. The lower density wood gave a poor bond index at high freeness (or low scattering coefficient) levels, and a large difference in scattering coefficients at high freenesses.

This data provides a potential mechanism for the low strength of the fast growth rate pine. For example, a high level of surface lignin could interfere with bond strength. The Klason lignin analysis of pulp samples from this project give an average 29.9% lignin for the fast growth rate pine, and 29.8% for slow growth rate pine. This is not enough to account for the change in bonding behavior. Differences in the distribution of lignin within the fiber wall could also influence the bond strength. A high lignin content in the S_1 and initial S_2 layer of the fast growth rate trees, would interfere with fiber bonding and give a low bond strength paper. At present, there is no data to support or refute this possibility but recent research in New Zealand has shown variations in cell wall lignin distributions that affect thermomechanical pulping of radiata pine.[19]

CONCLUSIONS

Fiber damage begins in the earliest stages of refining, and most of the fiber cleavage and much of the fiber wall damage supporting later fines generation has occurred by the time 200 to 300 kWh/ODT of specific refining energy has been applied. Similar results have been reported by others for samples collected at 500 kWh/ODT. In addition, wood type and refining conditions are found to create distinct differences in the rates at which fibers are liberated from the chip mass and broken in the refining process. Generally, the total coarse wood mass (R_{14}) breaks down at nearly the same rate for the three species evaluated, but at slightly different rates for the two refiner plate types. This rate can be increased considerably by refining at low moisture contents as observed with the initial spruce sample. Spruce and slow growth pine develop the long fiber fraction at a slower rate than the fast growth rate pine, but also have less long fiber reduction in extended refining than the fast growth rate pine. This results in the decrease in long fiber normally observed when refining plantation pine. The distribution of earlywood and latewood in the various wood particle and fiber size fractions does not confirm the earlier work showing evidence of preferential energy absorption in earlywood. Given the differences in specific energy between the two experiments (20 kWh/ODMT in the earlier experiments, 200kWh/ODMT in these experiments), this may be due to a change in refining mechanisms after the initial breakdown of wood. Handsheet data suggest the low density pine sample has a low bond strength which could be due either to a low specific bond strength, or a reduced bonded area. Freeness scattering relationship suggests the problem is low bond area.

REMAINING WORK:

All the work in this tasks has been completed. The identification of the low bond strength in low density pines needs to be evaluated to determine how much this contributes to the low strength of the pines. Project activity planned for FY 97/98 includes a determination of surface lignin contents of low and average density southern pine TMP fibers, and an evaluation of the freeness/surface area relationship for low and average density southern pines. Additional work is planned to evaluate the effect of impact intensity in early stage refining using the Defibrator D. Engineering work to install load cells to measure shear and compressive impacts in this device should be completed and the cells installed this year. Additional modifications planned for the Defibrator D include addition of variable drive speed capability and an improved chip feeding arrangement.

ACKNOWLEDGEMENTS:

Financial support for this project has been provided by the Institute member companies, and Newsprint South Corporation. Andritz Sprout-Bauer Inc. provided the three sets of refiner plates and waived half the cost of the pilot plant for the project.

Table 6. Results from optical microscopy of the chlorite holopulped Bauer McNett fractions

	Mesh size	% latewood	% Whole Earlywood	% Whole Latewood
Spruce	14	23	19	57
whole	28	33	14	51
	48	38	18	36
	200	38	2	8
Slow	14	13	0	6
pine	28	47	36	55
whole	48	49	15	24
	200	37	0	18
Fast	14	58	42	69
Pine	28	37	62	78
Whole	48	22	40	69
	200	29	3	21
Spruce	8	30	52	73
Inter.	14	32	47	52
	28	29	50	75
	100	38	14	20

	Mesh Size	% Latewood	% Whole Earlywood	% Whole Latewood
Slow	8	26	14	3
Pine	14	38	42	64
Inter.	28	47	28	47
	100	45	11	18
Fast	8	22	27	38
Pine	14	25	32	78
Int.	28	39	49	66
	100	45	24	47
Spruce	4	18	37	37
Small	14	29	35	32.7
	48	46	30	53
	100	51	7	19
Slow	4	39	29	48
Pine	14	35	35	35
Small	48	53	22	31
	100	53	6	6
Fast	4	8	26	23
Pine	14	20	13	30
Small	48	41	40	57
	100	31	5	13

REFERENCES

1. Hiller, C.H. and Brown, R.S., "Comparison of Dimensions and Fibril Angles of Loblolly Pine Tracheids Formed in Wet or Dry Growing Seasons" *American Journal of Botany,* **54**(4): 453-469(1967).

2. Jayne, B.A., "Wood Fibers In Tension" *Forest Products Journal,* **10**(6): 316-322(1960).

3. Page, D.H., El-Hosseiny, F., Winkler, K. and Bain, R., "The Mechanical Properties of

Single Wood-Pulp Fibres. Part 1: A New Approach" *Pulp and Paper Magazine of Canada,* **73**(8): 72-77(1972).

4. Hickey, K.L. and Rudie, A.W. "Preferential Energy Absorption by Earlywood in Cyclic Compression of Loblolly Pine" *Poster Presentations, 1993 International Mechanical Pulping Conference,* EUCEPA, Oslo, p 81-86.

5. Kennedy, R.W. and Ifju, G., "Applications of Microtensile Testing to Thin Wood Sections" *TAPPI J.,* **45**(9): 725-733(1962).

6. Ifju, G., "Within-Growth-Ring Variation in Some Physical Properties of Southern Pine Wood" *Wood Science*, **2**(1): 11-19(1969).

7. Biblis, E.J., "Transitional Variation and Relationships Among Properties Within Loblolly Pine Growth Rings" *Wood Science and Technology,* **3**: 14-24(1969).

8. St. Laurent, J.M., Rudie, A.W. and Shakhet, A.R., "Mechanical Pulping by Fractionation after Low Energy Refining" *Proceedings, 1993 TAPPI Pulping Conference,* TAPPI Press, Atlanta, p 95-99.

9. Wynn-Roberts, R.I., "Grinding Characteristics of Various Wood" *Technical Association Letters*, **XX**: 258(1937).

10. Kurdin, J.A., "Refiner Mechanical and Thermomechanical Pulping" in *Pulp and Paper, Chemistry and Chemical Technology,* 3rd. Edition, J.P. Casey, Ed., John Wiley and Sons, N.Y. p 211 (1980).

11. Yan, J.F., "Kinetic theory of mechanical pulping" *Tappi J.,* **58**(7): 156-158(1975).

12. Kano, T., Iwamida, T., and Sumi, Y., "Energy consumption in mechanical pulping" *Pulp and Paper Canada,* **83**(6): T157-T161(1982).

13. Strand, B.C., and Mokvist, A., "The application of comminution theory to describe refiner performance" *Preprints, 74th Annual Meeting of the Technical Section, CPPA,* B115-B121 (1988).

14. Rudie, A.W., Shakhet, A., Carter, B., and Griffey, J., "A chlorite holopulping method to evaluate strength changes in TMP" *Proceedings, 1995 International Mechanical Pulping Conference,* pp. 227-232 (1995).

15. TAPPI Standard method, T 233 cm-82.

16. Heikkurinen, A., Vaarasalo, J., and Karnis, A., "Effects of initial defiberization on the properties of refiner mechanical pulps" *Proceedings, 1991 International Mechanical Pulping Conference,* pp 303-319 (1991).

17. Rueckert, C.B., "Thermal imaging of fiber aggregates subjected to cyclic compression" IPST Annual Project Review, High Yield Pulping PAC, March, 1997.

18. Sinkey, J.D., "The development of high-yield pulp properties," *Preprints, 70th Annual Meeting CPPA,* pp. B75-B82(1984).

19. Donaldson, L.A., "Cell wall fracture in relation to lignin distribution and cell dimensions among three genetic groups of radiata pine" *Wood Science and Technology*, **29**: 51-63(1995).

Fundamentals of Brightness Stability

PROJECT SUMMARY

PROJECT TITLE: Fundamentals of brightness stability

PROJECT STAFF: A.J. Ragauskas, L. Allison

FY 97 BUDGET: $72,000

DIVISION: Chemical and Biological Sciences

PROJECT NUMBER: F014

OBJECTIVE:

Research objectives are directed at investigating the fundamental chemical reactions that are initiated when high-yield pulps are photolyzed. As our knowledge of the photoxidation of mechanical pulp increases, methods to eliminate or significantly retard the yellowing process will be pursued.

GOAL: Increase the usefulness of high-yield fibers.

CURRENT RESULTS:

Research efforts over this past fiscal year have accomplished the four research goals established in the spring 1995 PAC, including:

1. Determine photostabilization effects of carrier molecules and radical scavengers with Fluorescent Whiting Agents (FWA).

   Accomplishment: The photostabilization effects of FWAs was examined at several dose response levels and under most circumstances beneficial photostabilization effects were observed. The use of carrier substrates, such as polyethylene glycol (PEG), were shown to extend the

photostabilization benefits of FWA. Research studies also demonstrated synergistic effects could be achieved when a FWA agent was employed in the presence of PEG or polytetrahydrofuran and an antioxidant.

2. Study failure mechanism of FWA applied on BCTMP.

Accomplishment: The photostabilization effects of a FWA applied onto BCTMP-kraft hand sheets was evaluated over prolonged time periods prior to photolysis. The effects of light-dark cycling on treated hand sheets was also studied. In both cases, storage of FWA-treated hand sheets did not detrimentally impact optical properties.

3. Examine the effects of additive application technology for FWA applied onto BCTMP-kraft hand sheets and photoaged.

Accomplishment: Preliminary studies directed at applying a FWA and secondary additive onto test sheets in the form of a coating mixture were performed. Employing percol as a carrier, mixtures of FWA and antioxidant were applied onto BCTMP-kraft hand sheets. The treated hand sheets were irradiated and data analysis suggested that the photostabilization effects of the FWA was not detrimentally affected by applying the additives onto hand sheets by a coating procedure.

4. Prepare a review article summarizing past research accomplishments in brightness reversion.

Accomplishment: A Membership report on project F014 was written and distributed to IPST member companies

FUTURE PROPOSED ACTIVITY:

Proposed studies for the next fiscal year will attempt to advance the photostabilization effects developed to date and develop technologies suitable for mill application. These goals include:

1) Prepare coated BCTMP/kraft test sheets with FWA, polymer and antioxidant and examine photoreversion properties.

2) Examine role of clay and starch in brightness stabilization coating technology.

3) Selective acylation of BCTMP to retard brightness reversion.

Table 1: Proposed future research activities.

Research Goal	FY 1997-98 Research Schedule: 1st Quarter	2nd Quarter	3rd Quarter	4th Quarter
• Coating Studies	**	**		**
• Influence of clay and starch			**	
• Pulp modification		**	**	**

RELATED RESEARCH ACTIVITY:

1. NSF funded research activities in "Stabilization of Mechanical Pulp Against Color Reversion" are ongoing. Research studies to-date have defined the mechanisms by which thiol and disulfide additives photostabilize mechanical pulp. We have also discovered a new class of photostabilization additives, thio-sulfinates, that are as effective as thiols at retarding reversion and do not have the malodorous properties of thiols.

2. Ragauskas was successful in securing research funds from USDA to study "Fundamentals of Lignocellulosic Photostabilization Chemistry." This project will determine the fundamental chemical pathways involved in the

degradation of UV-additives applied onto mechanical pulp.

3. With the support of the Gunnar Nicholson Exchange Program, a new research project directed at evaluating the use of acylation technologies for retarding brightness reversion will be initiated.

PROJECT REPORT

PROJECT NAME: Fundamentals of brightness stability

INTRODUCTION: Advances in mechanical pulping and bleaching have significantly improved the quality of this valuable fiber resource. Unfortunately, commercial use of these pulps is limited due to their well known yellowing properties. Although reversion can be initiated either by heat or light, the latter process is frequently the dominant contributor to the discoloration of mechanical pulps and as a result has been the focus of research studies at IPST.

Past studies at IPST have identified several lignin chromophores involved in the photoyellowing of mechanical pulp. Over the last few years, research efforts at IPST have been directed at utilizing the advances in photoyellowing chemistry to develop new brightness stabilization additives. Early studies in this field examined the use of novel antioxidants and UV-absorbers and demonstrated distinct photostabilization benefits.

Subsequent studies demonstrated that synergistic effects were possible if the use of UV-absorbers and antioxidants were used in combination. Recent studies, summarized in last year's PAC report and the subsequent Membership Report, demonstrated that fluorescent whitening agents (FWA) provided very distinct benefits at retarding the overall rates of brightness reversion. The most significant accomplishment from last years study was the ability to retain a 25% BCTMP - kraft test sheet above Tappi brightness 87 for in excess of 20 days while applying a 1% charge of FWA as shown in Figure 1.

Figure 1: Photoreversion of 75% softwood kraft and 25% BCTMP handsheets treated with Tinopal, Blankopher, Phorwite P, and Phorwite UW.

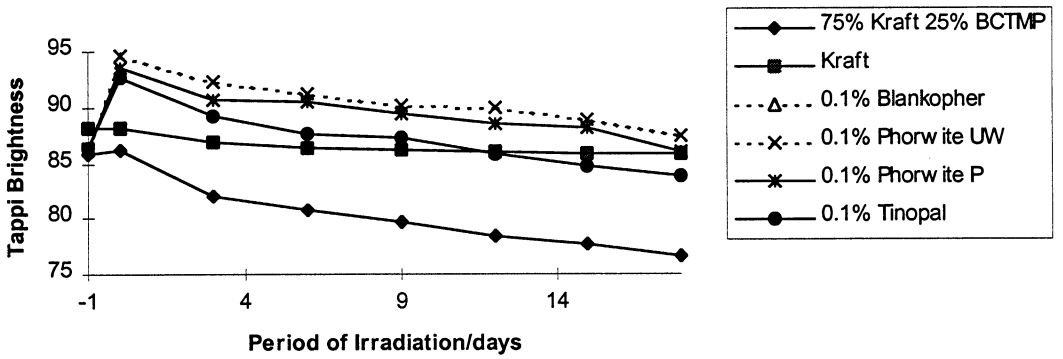

This year's research goals included:

1. Research the photostabilization effects of carrier molecules and radical scavengers with FWA.

2. Study the failure mechanism of FWA applied on BCTMP and irradiated with office lighting.

3 Examine the effects of additive application technology for FWA applied onto BCTMP-kraft hand sheets and photoaged.

REVIEW OF FY 1996-97 ACTIVITY.

Goal 1: Photostabilization effects of FWA and co-additives.

Based on the previous year's investigation, Tinopal and Phorwite UW appeared to be two of the most promising FWA agents studied the past fiscal year. To fully evaluate the potential application of Phorwite UW as an photostabilization agent, test sheets of hardwood BCTMP were prepared and the effect of the FWA was accessed at various application levels with and without polyethylenegylcol (PEG).

Figures 2 and 3 summarize the photoaging results recorded for BCTMP test sheets treated with varying amounts of Phorwite UW and PEG when irradiated with office lights. Although the absolute rates of brightness reversion are slightly diminished, it is important to note that the addition of the FWA can increase the apparent brightness of the hand sheet approximately 7 TAPPI brightness points. The most beneficial application level is between 1.0 - 1.5% charge. At these charge levels, the use of 1% PEG was found to improve the overall optical properties of the treated hand sheets. To further evaluate the photoyellowing properties of UW treated test sheets, the overall rates of brightness reversion were monitored with the fluorescent component experimentally removed. Figure 4 and 5 summarizes these measurements and the results of this analysis suggest that the FWA is most effective at retarding the overall rates of brightness effects of BCTMP after approximately 20 days of irradiation.

Figure 2: Photoaging effects of 100% BCTMP Hand sheets Treated with 0.1 - 1.5% Phorwite UW

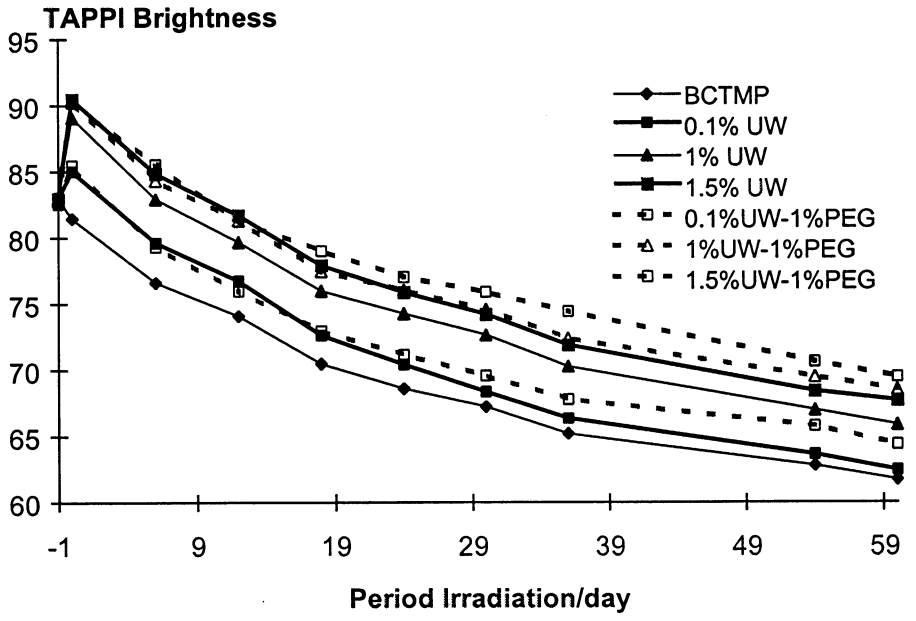

Figure 3: Photoaging effects of 100% BCTMP Hand sheets Treated with 2.0 - 4.0% Phorwite UW

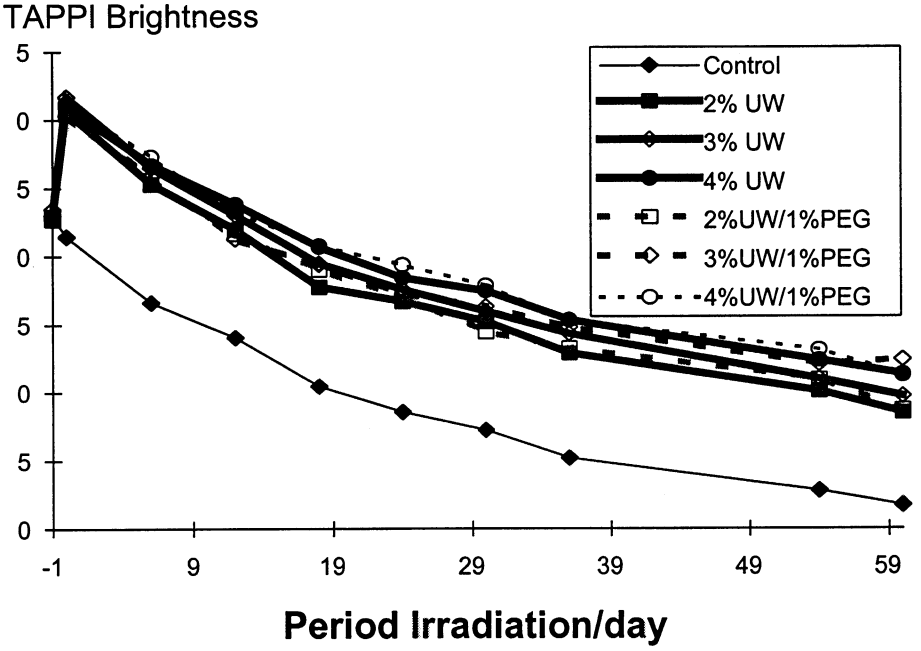

Figure 4: Photoaging properties of 100% BCTMP hand sheets treated with 0.1 - 4.0% Phorwite UW. Brightness values determined without fluorescence.

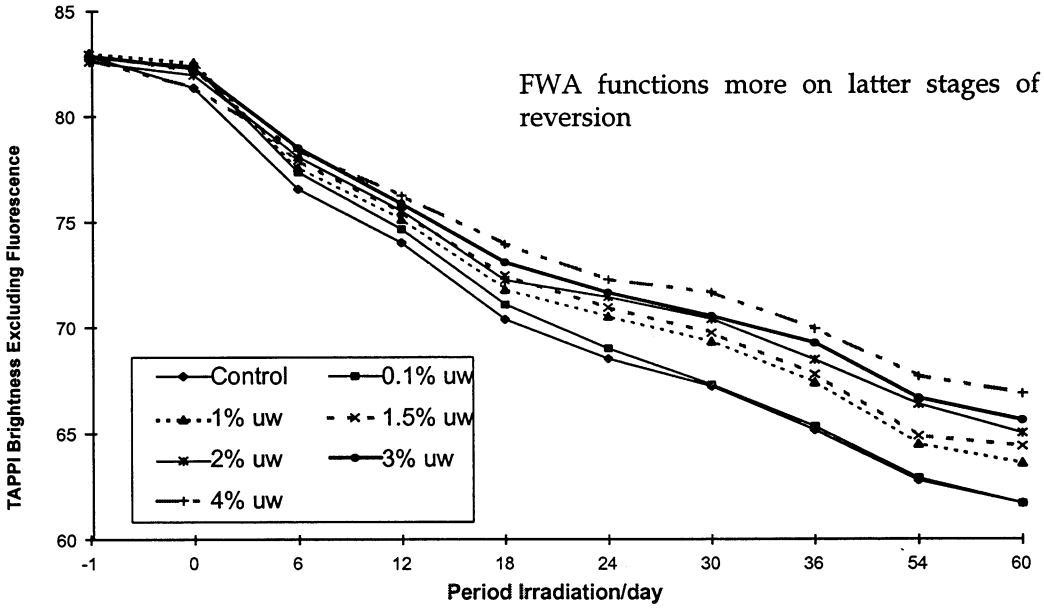

Figure 5: Photoaging properties of 100% BCTMP hand sheets treated with 0.1 - 4.0% Phorwite UW and 1.0% PEG. Brightness values determined without fluorescence.

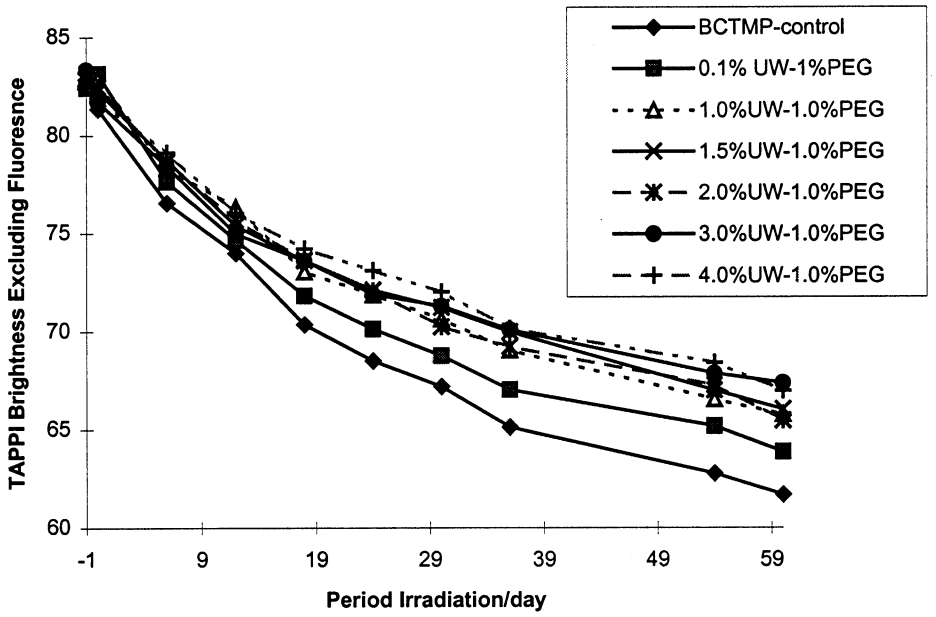

As a result of the beneficial reversion properties observed for BCTMP test sheets, the effectiveness of Phowite UW with and without PEG was examined on test sheets made of 75% hardwood kraft and 25% hardwood BCTMP. The results of these photoaging studies were monitored by TAPPI brightness with and without fluorescence, as summarized in Figures 6 and 7.

Figure 6: Photoaging properties of 25% BCTMP-kraft hand sheets treated with 0.1 - 4.0% Phorwite UW and 1.0% PEG. Brightness values determined without fluorescence.

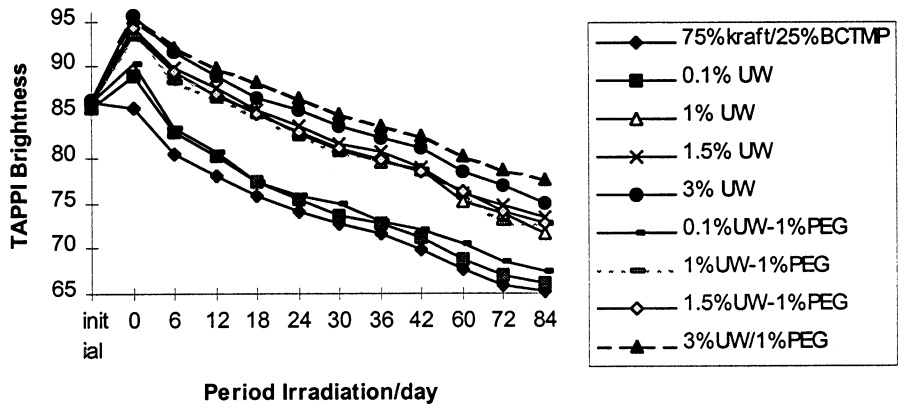

Note: 0.1%, 1.0%, 1.5%, 2.0%, 3.0%, 4.0% charges of UW was applied onto test sheets with and without PEG representative data is provided in Fig. 6.

Figure 7: Photoaging properties of 25% BCTMP-kraft hand sheets treated with 0.1 - 4.0% Phorwite UW and 1.0% PEG. Brightness values determined without fluorescence.

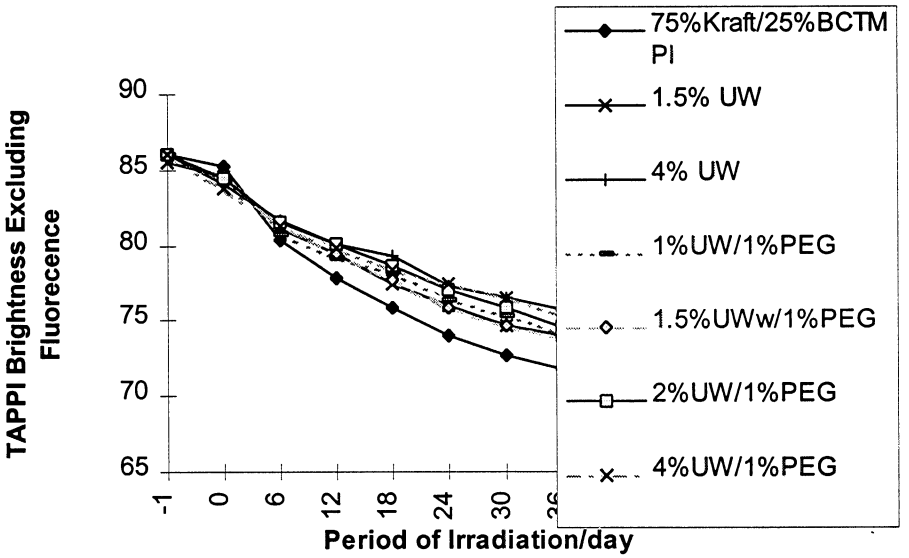

Note: 0.1%, 1.0%, 1.5%, 2.0%, 3.0%, 4.0% charges of UW were applied with and without PEG, representative data is provided in Fig. 7.

The results of these studies indicated that the photoaging properties of FWA treated BCTMP and 75% kraft-BCTMP test sheets exhibited comparable photoyellowing properties.

In response to PAC recommendations, the photoreversion properties of FWA treated BCTMP, kraft, and 25% BCTMP-kraft test sheets were further examined under natural sunlight conditions. The results of these investigations are summarized in Figures 8 - 11. The results from the solar photoaging studies suggest that the reversion properties previously observed under continuous office lighting are applicable to solar photoaging.

Figure 8: Solar photoaging properties of BCTMP-kraft hand sheets treated with 1.0% Phorwite UW, TAPPI brightness measurements.

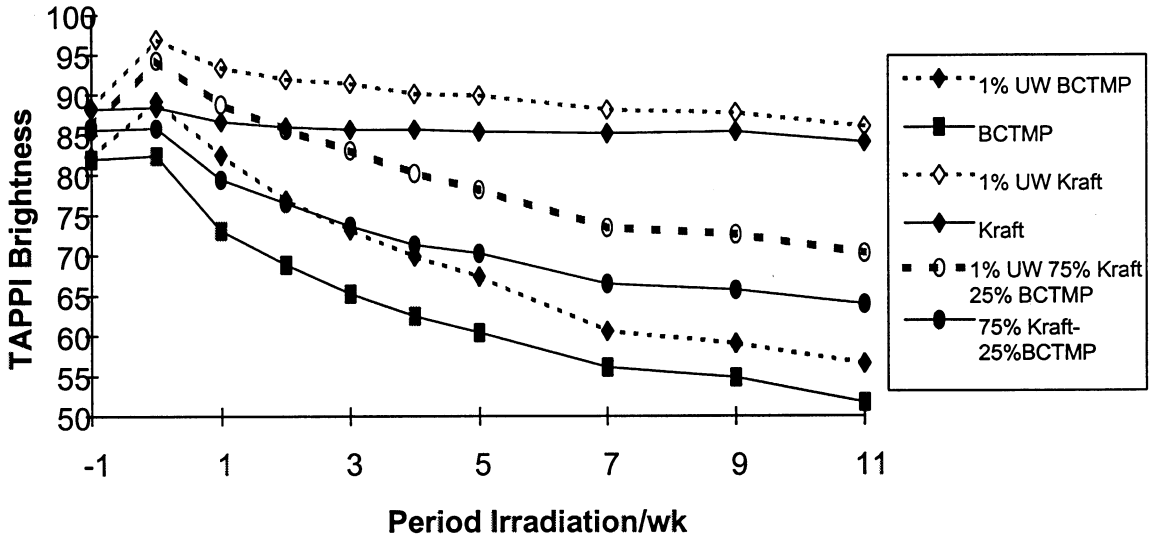

Figure 9: Solar photoaging properties of BCTMP-kraft hand sheets treated with 1.0% Phorwite UW, L* measurements.

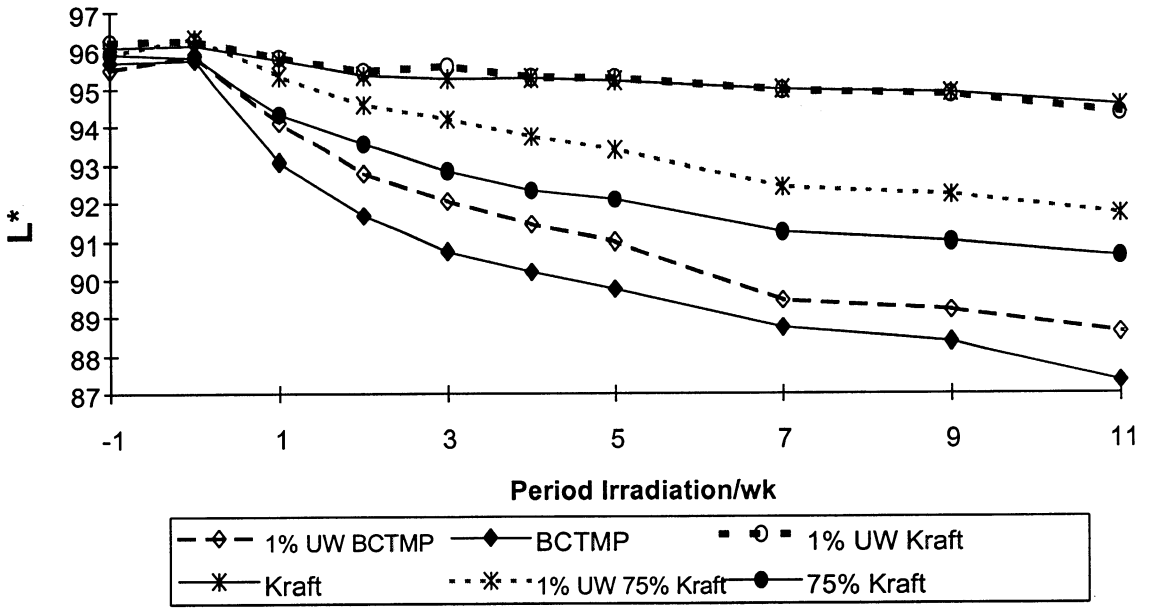

Figure 10: Solar photoaging properties of BCTMP-kraft hand sheets treated with 1.0% Phorwite UW, a* measurements.

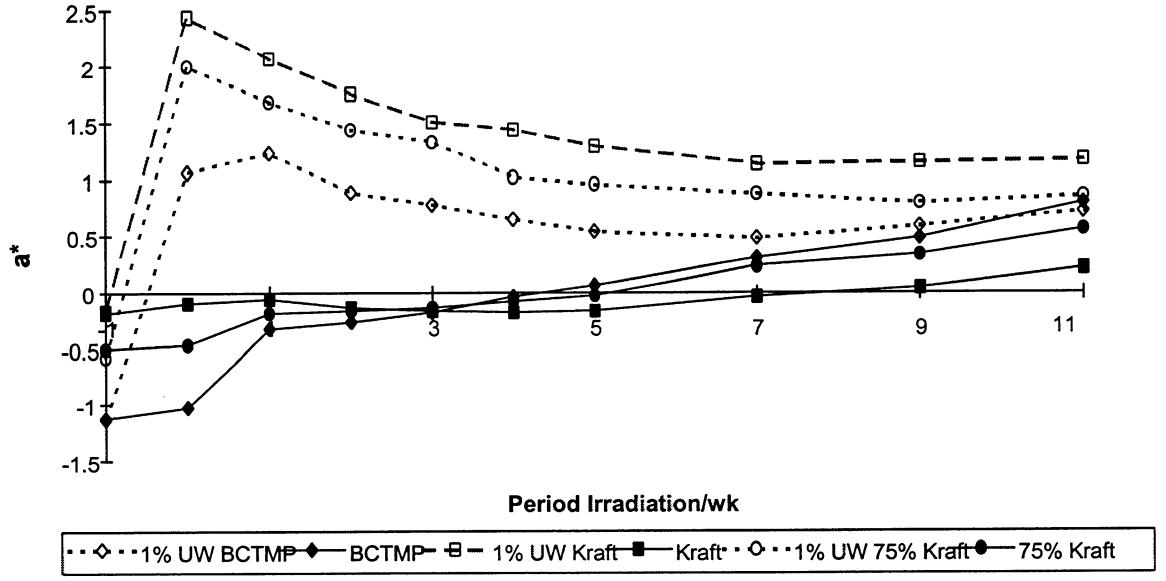

Figure 11: Solar photoaging properties of 25%BCTMP-kraft hand sheets treated with 1.0% Phorwite UW, b* measurements.

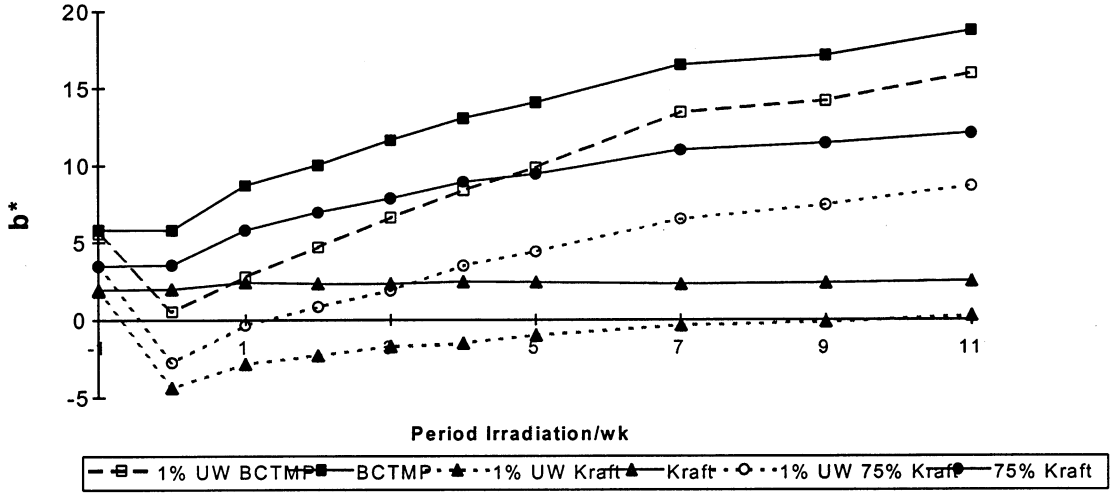

Synergistic Photostabilization Effects: The photostabilization effects of Tinopal with a secondary additive applied onto 25% BCTMP-kraft test sheets was explored using polyethylene glycol, polytetrahydrofuran, ethylenebisthiopropinate, methylenebisthiopropionate and mercaptoacetic acid (see Fig. 12).

Figure 12: Photostabilization additives.

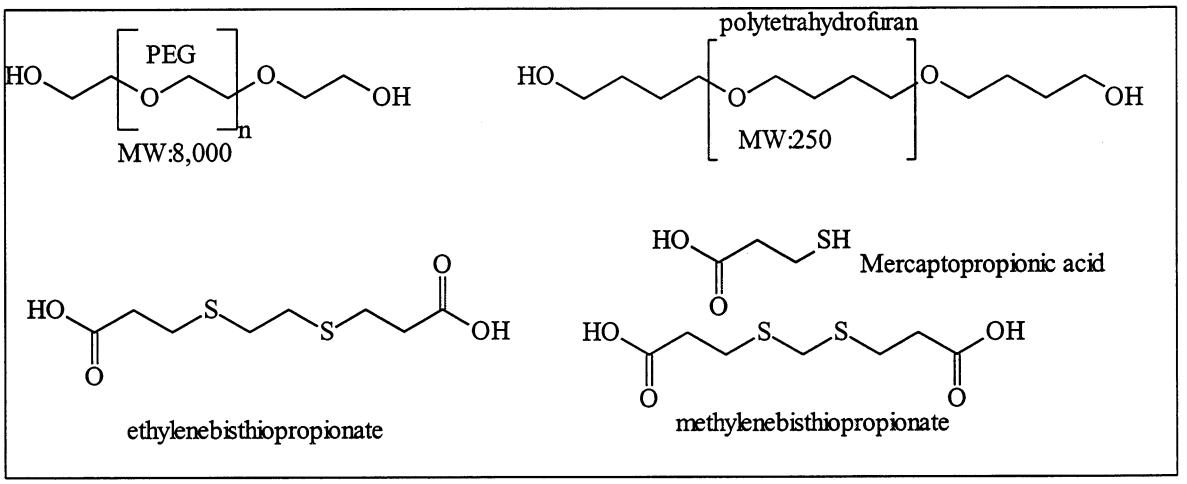

Long-term photoaging properties were determined using continuous office lighting for 39 days and these results are summarized in Figure 13-19. The results of

Tappi brightness analysis for the treated and untreated hand sheets are given in Figure 13.

Figure 13: Photoreversion[1] properties of 25% BCTMP-kraft hand sheets treated with 1.0% Tinopal, 1.0% PEG, 3.3% polytetrahydrofuran, 1.0% ethylenebis-thiopropinate, 1.0% methylenenbisthiopropinate, and 0.5% Mercaptopropinate acid.

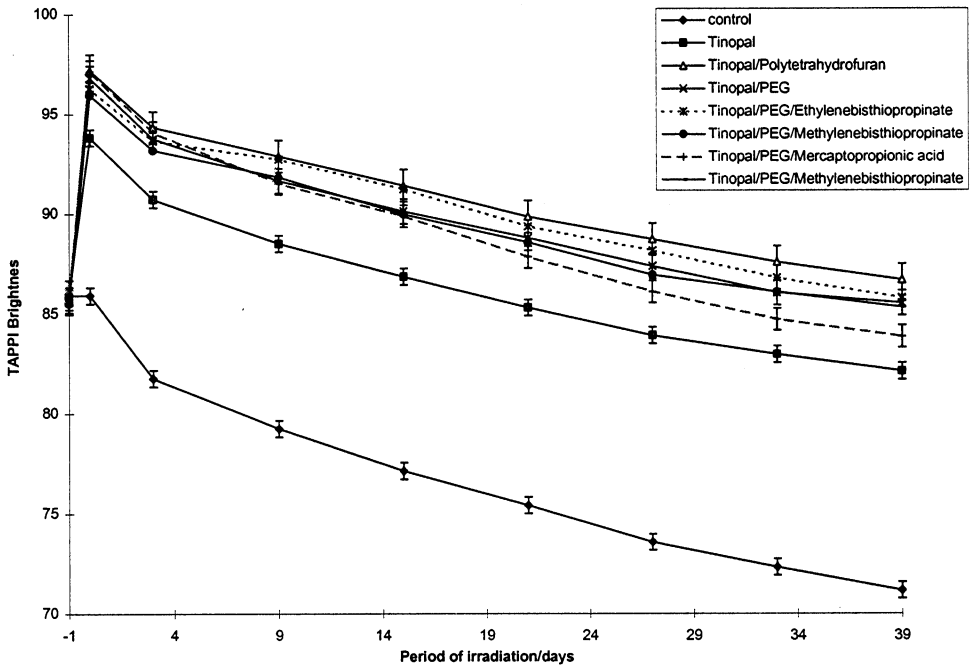

[1]all hand sheets were continuously photolyzed under office lights.

The addition of Tinopal does elevate the initial brightness values, such that after 24 days of continuous irradiation the treated hand sheets retain a +85 brightness. Nonetheless, the treated hand sheets also suffer brightness reversion, although it appears that test sheets treated with Tinopal and polytetrahydrofuran or Tinopal-polyethylene gycol-ethylenebisthiopropionate suffer the least amount of reversion. Table 2 summarizes the loss in brightness values for the treated and untreated hand sheets after 14 and 39 days of continuous irradiation.

Table 2: Tappi brightness loss data for untreated and treated 25% BCTMP-kraft hand sheets after 14 and 39 days of continuous irradiation.

TAPPI Brightness loss for treated BCTMP-kraft hand sheets

Period of Irradiation	Untreated	Tinopal	Tinopal/polytetrahydrofuran	Tinopal/ PEG	Tinopal/PEG/ Ethylenebisthiopropinate	Tinopal/PEG/ Methylenebisthiopropinate
14 days	8.8	7.0	5.8	6.7	5.1	6.0
39 days	14.8	11.7	10.5	11.3	10.5	10.6

The largest benefits from the additives is due to the application of Tinopal the use of polytetrahydrofuran or PEG provide a secondary benefit. The overall reduction in the rates of brightness reversion are further illustrated by measuring the overall rates of brightness reversion excluding the fluorescent component of brightness, as shown in Figure 14. These results further demonstrate the value of employing an optical brighter to reduce the overall rates of brightness reversion.

To complete the optical analysis of the hand sheets examined in Figures 13 and 14, we also determined the L*a*b* values for the test sheets during reversion and these results are summarized in Figures 15 -17. The most notable effect of by this analysis is the substantial reduction in the b* values for the Tinopal treated hand sheets during brightness reversion.

Figure 14: Fluorescent excluded photoreversion[1] properties of 25% BCTMP-kraft hand sheets treated with 1.0% Tinopal, 1.0% PEG, 3.3% polytetrahydrofuran, 1.0% ethylenebisthiopropinate, 1.0% methylenenbisthiopropinate, and 0.5% Mercaptopropinate acid.

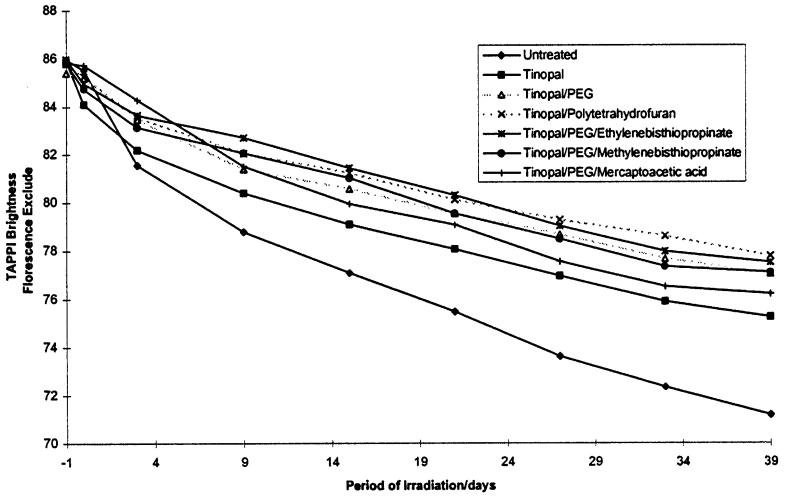

Figure 15: L* photoreversion[1] properties 25% BCTMP-kraft hand sheets treated with 1.0% Tinopal, 1.0% PEG, 3.3% polytetrahydrofuran, 1.0% ethylenebisthiopropinate, 1.0% methylenenbisthiopropinate, and 0.5% Mercaptopropinate acid.

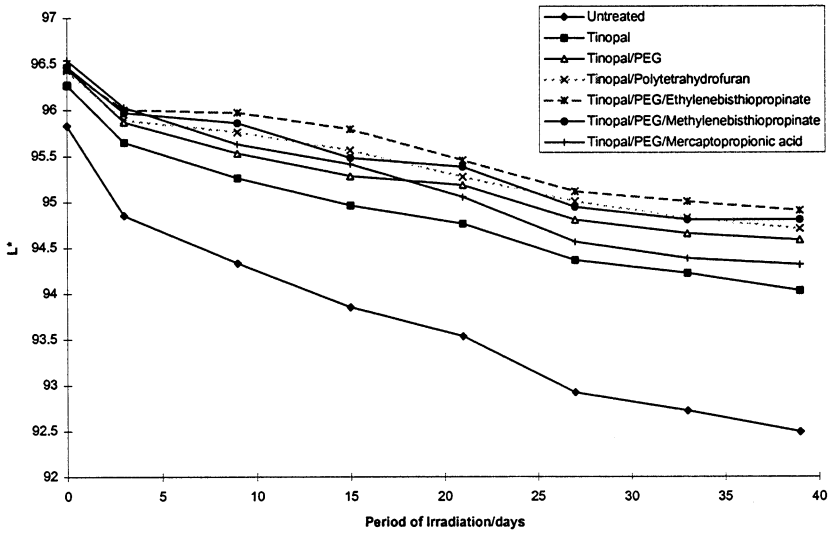

Figure 16: a* photoreversion[1] properties of 25% BCTMP-kraft hand sheets treated with 1.0% Tinopal, 1.0% PEG, 3.3% polytetrahydrofuran, 1.0% ethylenebisthiopropinate, 1.0% methylenenbisthiopropinate, and 0.5% Mercaptoacetic acid.

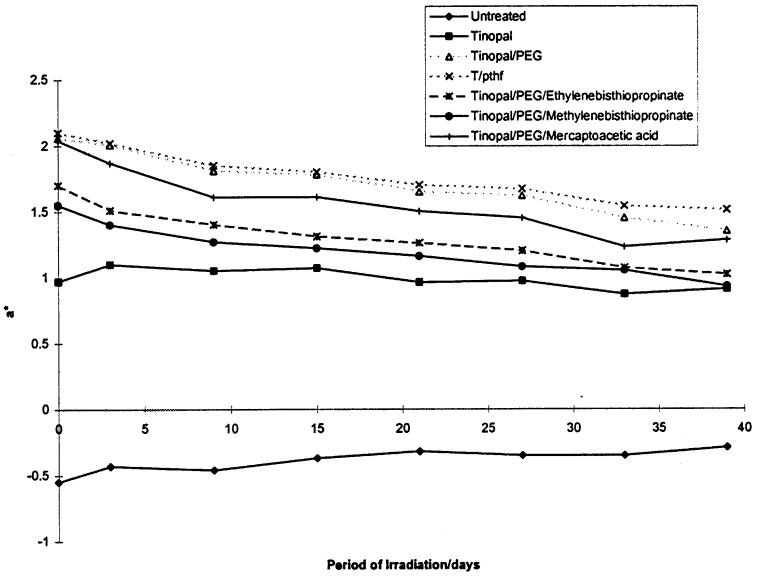

Figure 17: b* photoreversion[1] properties of 25% BCTMP-kraft hand sheets treated with 1.0% Tinopal, 1.0% PEG, 3.3% polytetrahydrofuran, 1.0% ethylenebisthiopropinate, 1.0% methylenenbisthiopropinate, and 0.5% Mercaptopropinate acid.

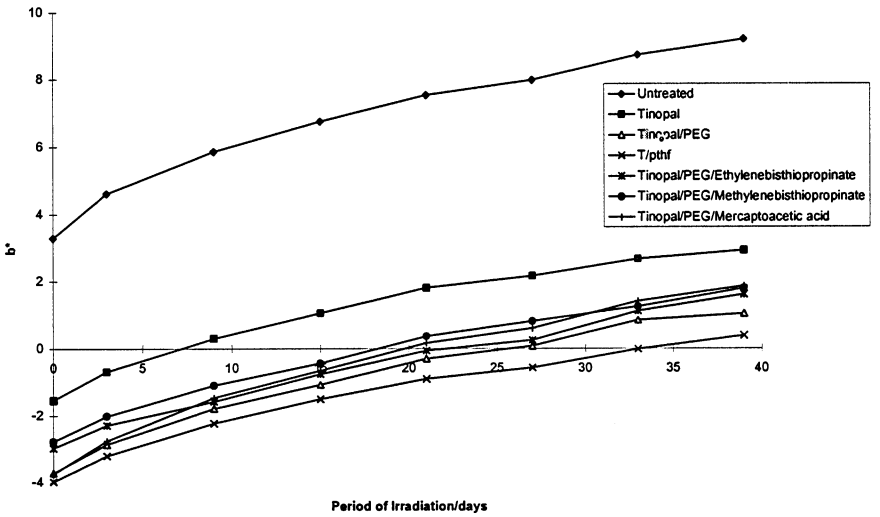

The effectiveness of UW with co-additives was also examined this past fiscal year, as summarized in Figure 18.

Figure 18: Photoreversion[1] properties of 25% BCTMP-kraft hand sheets treated with 1.0% UW, 1.0% PEG, 3.3% polytetrahydrofuran, and 1.0% ethylenebisthiopropinate.

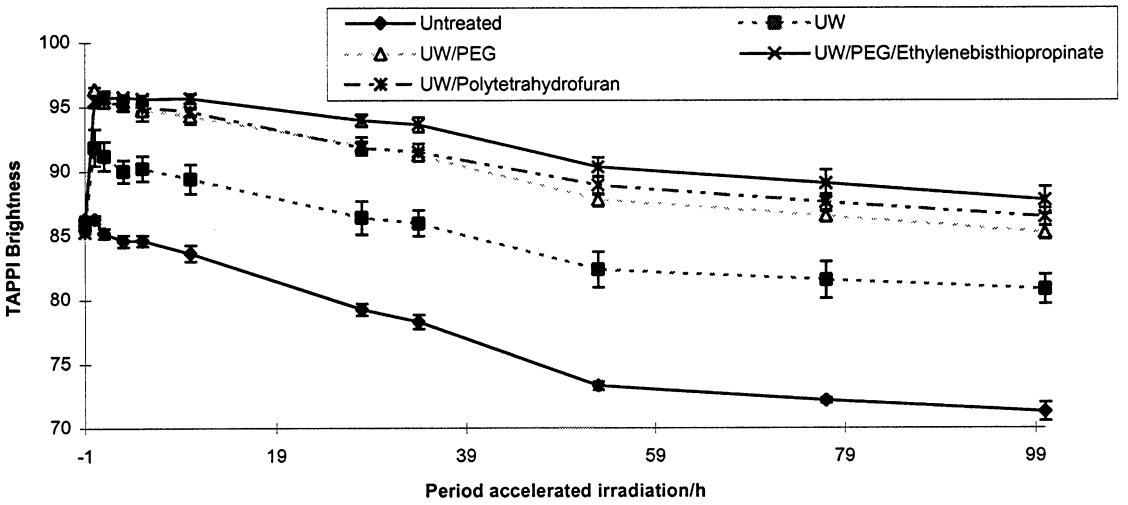

[1]see Fig. 19 for chemical structures of Tinopal and Phorwite UW.

Figure 19: Molecular structure of Tinopal and Phorwite UW.

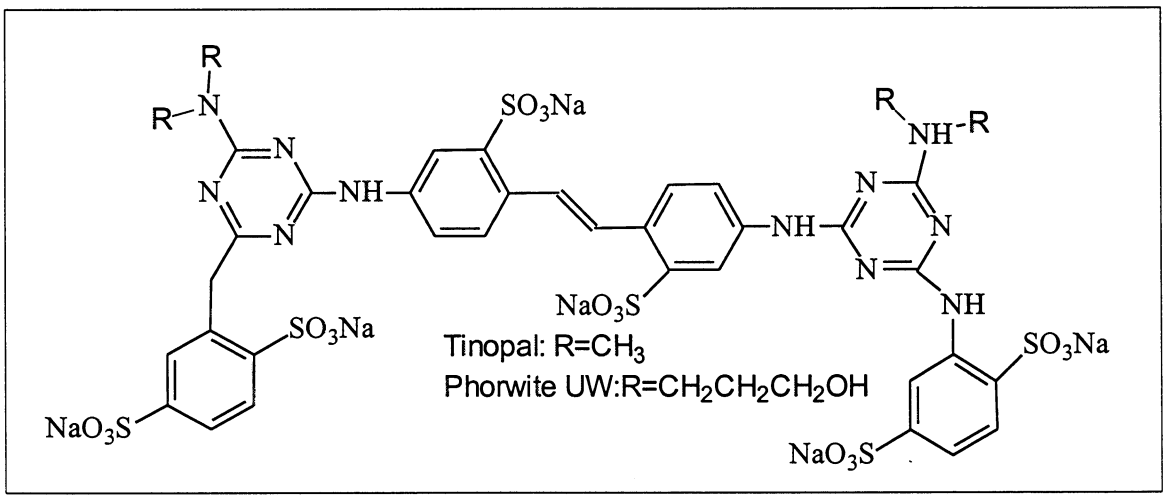

Goal 2: Failure mechanism of FWA applied on BCTMP.

Past investigations into photostabilization of mechanical pulp have demonstrated that some additives were detrimentally impacted by long term storage prior to photolysis. In response to these concerns, FWA treated BCTMP hand sheets were stored in the dark and brightness values were periodically recorded (see Fig. 20). The results of these studies indicated that FWA applied onto BCTMP will not detrimentally impact the test sheet.

Figure 20: Thermal reversion of BCTMP test sheets treated with FWA.

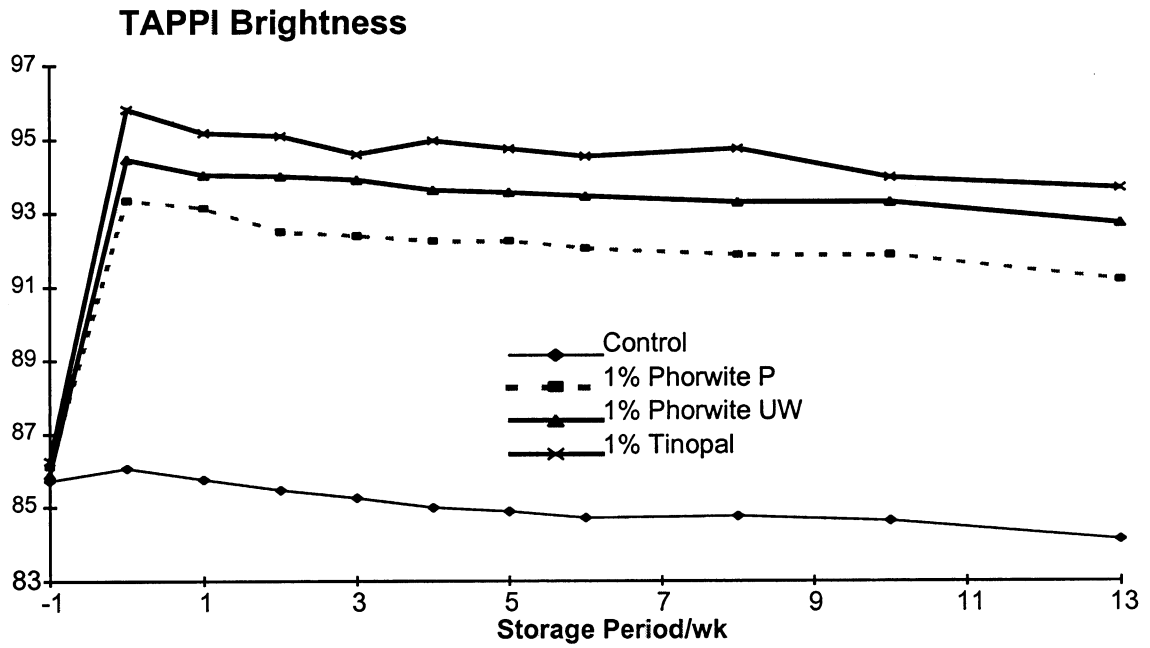

As a follow-up to the previous PAC review, the photoaging of FWA treated 25% BCTMP-kraft test sheets was evaluated against a periodic exposure to office lighting. The results of the light-cycling tests are summarized in Figure 21 and 22. This data suggests that the FWA-treated hand sheets do not exhibit any detrimental effect due to periodic exposure to light.

Figure 21: Solar photoaging properties of BCTMP-kraft hand sheets treated with 1.0% Phorwite UW, TAPPI brightness measurements.

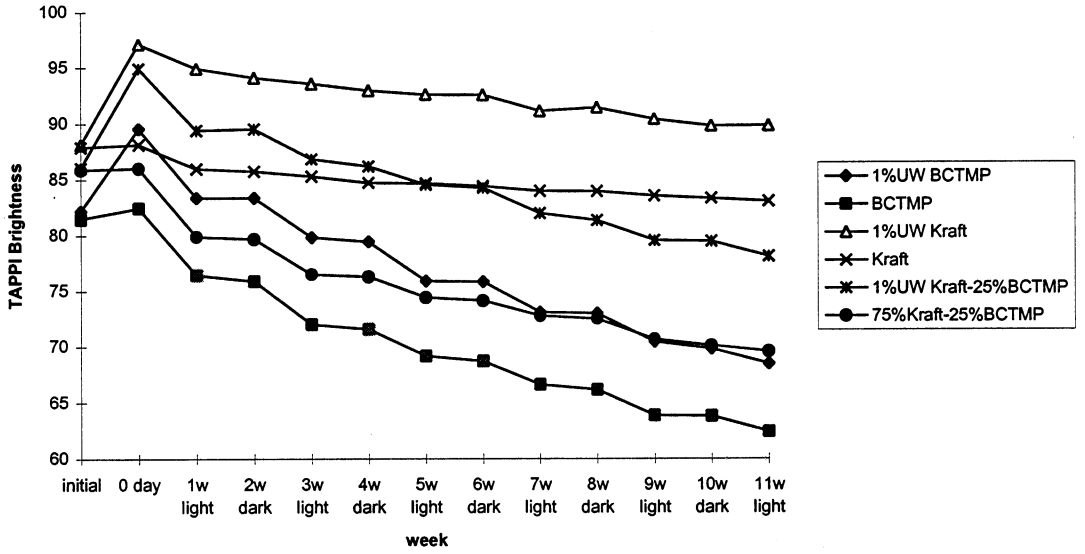

Figure 22: Solar photoaging properties of BCTMP-kraft hand sheets treated with 1.0% Phorwite UW, TAPPI brightness measurements excluding fluorescence.

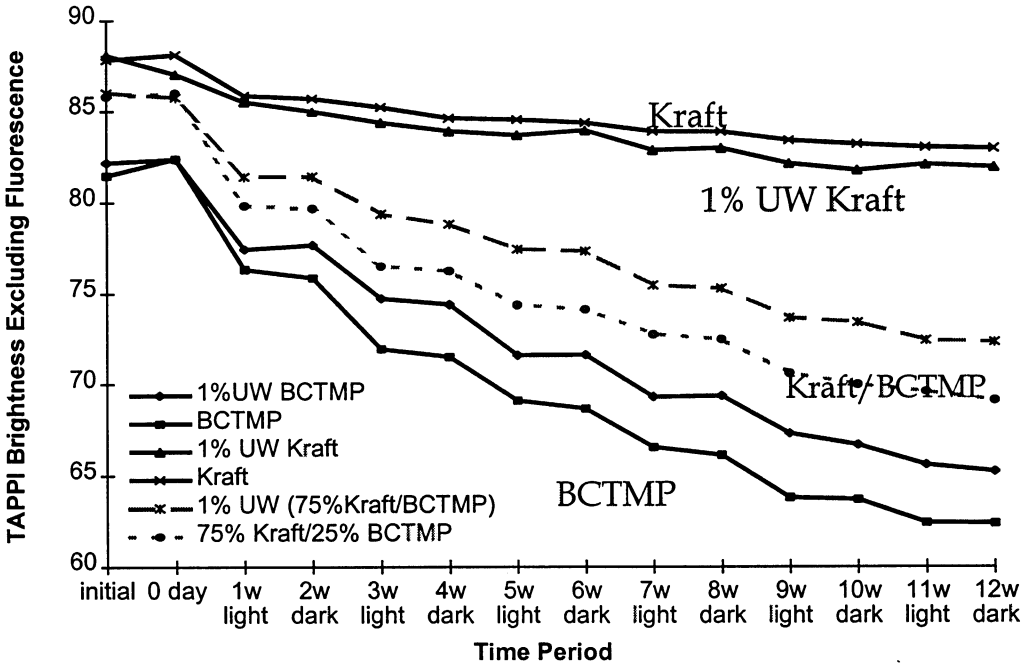

Goal 3: Additive application technology. The final research issue for this fiscal year was to examine the influence of "mill applicable" application technologies for additives examined to date. As an initial investigation a series of 25%BCTMP-kraft were coated with 0.01% percol 175, 3.3% polytetrahydrofuran, 1.0% PEG, and 1.0% ethylenebisthiopropinate. The coated hand sheets were placed in a light box containing a series of office lights and reverted under accelerated conditions. The results of these studies are summarized in Figure 23.

Figure 23: 25% BCTMP-kraft hand sheets treated with 0.01% Percol 175, 1.0% Tinopal, 1.0% PEG, 3.3% polytetrahydrofuran, 1.0% ethylenebisthiopropinate, 1.0% methylenenbisthiopropinate, and 0.5% Mercaptopropinate acid

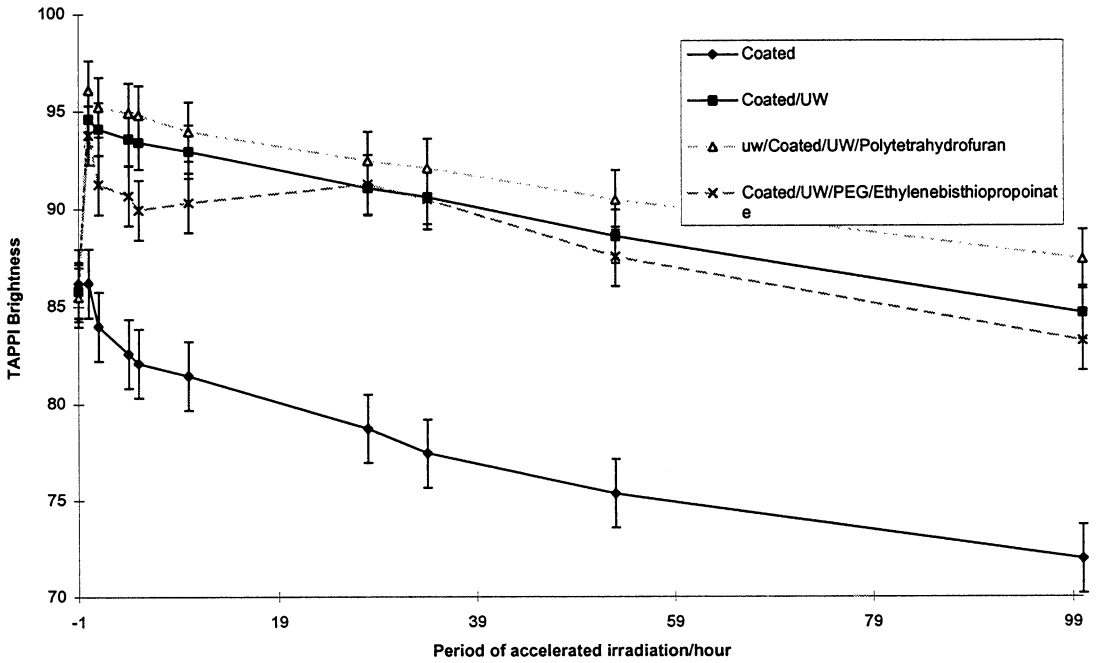

It is interesting to note that coating additive percol 175 does not impair the fluorescent whitening properties of the optical brightening agents. The use of Phorwite UW, PEG and ethylenebisthiopropinate exhibited a unique reversion property. Within the first few days of application, the test sheets exhibited a sharp drop in brightness of a few points and then remained relatively constant for the

next 20 days. **If this process can be repeated under ambient photoyellowing conditions, it appears that this additive technology can yield a +87 pulp that is relatively photostable for an extended time period. This has been the long term goal of this project and other researchers for the last two decades.**

EXPERIMENTAL

Materials: All chemicals including Tinopal, Phorwite UW, PEG, polytetrahydrofuran, methylene bisthiopropionate and ethylene bisthiopropionate were commercially purchased and used as received. Commercial hardwood BCTMP (93% yield) prepared from aspen, using hydrogen peroxide for both the chemical pretreatment and bleaching was employed for all studies in this report. A commercial hardwood kraft pulp fully bleached was used as received.

Hand sheets: 1.20 gr hand sheets were prepared following Tappi procedure T 205.

Additive Application Method: With the exception of the coating experiments, all additives were applied onto hand sheets in aqueous solution (10 ml/hand sheets) using an aerosol nebulizer. The resulting hand sheets were then air dried under restraint and optical properties measured their after.

Optical Measurements: All optical measurements were made according to standard TAPPI testing methods: TAPPI Brightness with and without fluorescence : Tappi 452; L*a*b*: T 527; and Scattering/Absorption Coeff.: T 220.

Photoaging Testing Procedure: Ambient photoaging experiments were performed by placing hand sheets ca. 9' removed from a series of office lights. Solar aging was performed by placing test sheets against a desk facing the

south-side of IPST. Accelerated office lighting aging was accomplished by placing hand sheets on a rotating metal frame within a cylindrical drum containing eight Sylvan F8T5/WW warm white office lights.

Coating Experiments: A series of 1.20 gr hand sheets prepared from 75% kraft and 25% BCTMP were coated with a viscose solution of 0.01% percol 175, and 1.0% Phorwite UW . Additional additives utilized 1.0% PEG, or 3.3% polytetrahydrofuran, or 1.0% ethylene bisthiopropionate. The treated hand sheets were dried under restraint and used for accelerated office aging conditions.

General Experimental Notes:

a) All reported Tappi brightness values are apparent brightness values, therefore, the results reported for hand sheets treated with fluorescent whitening agents contain the fluorescent component from the additive unless stated otherwise.

b) Each reversion figure shown in this report has a time -1 Tappi brightness value, this number is the Tappi brightness prior to addition of the additive. Tappi brightness values reported at time 0 are the values just prior to irradiation.

c) All reversion tests employed 1.20 gram TAPPI hand sheets unless stated otherwise.

CONCLUSIONS

The use of commercial fluorescent whitening agents to retard brightness reversion is one of the most successful technologies studied in this program. The use of

these additives separately or in concert with co-additives offers the opportunity to retain +85 Tappi brightness values for in excess of three weeks. These benefits can be incurred employ technologies readily available to most modern mill operations.

RELATED STUDIES

With the support of the Mechanical PAC committee Ragauskas was able to secure additional funding from USDA to examine several important fundamental reversion research issues that will allow the dues funded project to move ahead at an accelerated rate. Summarized below is the project summary statement for this project.

Project: Title: **Fundamentals of Lignocellulosic Photostabilization Chemistry**

Project Summary:

The principal factor limiting further use of mechanical pulp is its well-known tendency to undergo photoyellowing. The research goal of this proposal is to develop a fundamental understanding of the chemical mechanisms that contribute to the photostabilization of mechanical pulps. These results will be employed to develop the next generation of effective photostabilization strategies for mechanical pulps. This will permit enhanced usage of this valuable fiber resource and thereby improve wood utilization practices for the industry.

This research goal will be accomplished by studying the fundamental mechanisms by which UV-screens retard the overall rates of photoyellowing of mechanical pulps, research issues include:

- Failure mechanisms of UV-screens;
- Lignocellulosic reactions that contribute to the failure of photostabilization strategies.

These research objectives will be determined by characterize the lifetime of UV-screens applied onto mechanical pulps and establishing their mechanisms of decomposition. This will be accomplished utilizing advanced HPLC, GC/MS and NMR methods. Lignocellulosic reactions that consume photostabilization additives or contribute to photoyellowing will be explored employing chemically modified mechanical pulps and the use of solid-state ^{31}P NMR of oxyphosphorylated mechanical pulp. The results of these fundamental studies will be employed to design new UV-screens with improved photostabilization properties.

Project: Title: **Acylation Technologies for Retarding Brightness Reversion**

Project Summary: Recent studies in Europe have shown that the acylation (see eq. 1) of lignin can effective retard the overall rates of brightness reversion.

eq. 1) $PhOH + Ac_2O \longrightarrow PhOAc$

Although this technology is not yet cost-effective, the use of acetic anhydride at low-charges has substantially dropped the cost of this technology. With the financial support of the Gunnar Nicholson Exchange Program, Dr. M. Paulsson will be arriving at IPST this summer to further pursue this avenue of brightness stabilization research. Project goals will include:

- Establishing the mechanisms of photostabilization for acylated BCTMP pulps;
- Application of photostabilization additives with acylated BCTMP pulps;
- Use of cross-linking acylation additives for strength and brightness stabilization benefits.

The results of these studies are anticipated to lead to further improvements in the brightness stabilization technologies developed at IPST for mechanical pulps.

Thermal Imaging of Fiber Aggregates Subjected to Cyclic Compression

PROJECT SUMMARY

PROJECT TITLE: **Evaluation of Strain in Earlywood and Latewood of Loblolly Pine in Cyclic Compression**

PROJECT STAFF: **Cheryl B. Rueckert (Ph.D. candidate)**

BUDGET: **Ph.D. Research**

DIVISION: **C&BSD**

PROJECT NUMBER: **Ph.D. Research**

OBJECTIVE: Investigate the distribution of strain between earlywood and latewood in fiber aggregates subjected to cyclic load to simulate a disk refiner. The hypothesis is that the earlywood fibers will be preferentially strained and have a larger temperature increase than the latewood fibers.

GOALS: Evaluate impact of low frequency cyclic compression on fiber strain, using curl index.

ABSTRACT:

Previous research has shown that the earlywood portion of the annual growth ring appears to receive the majority of the energy in the early stages of chip refining. This study is attempting to determine if preferential energy absorption extends further into the refining process. Studies are being carried out on fiber aggregates, simulating a fiber floc in the coarse bars of a refiner. The fiber aggregates are cyclically compressed at 10, 30, 50, and 100 hertz. Curl index, measured after various predetermined compression cycles, is used as an index of strain (an indirect measurement of energy applied to the fibers). The change in the curl indices of the earlywood and latewood fibers are then compared to determine if there is preferential energy absorption due to fiber type. The temperature change of individual fibers is a the direct measurement of energy absorption. Fiber temperatures have been measured with infrared thermography and these results largely confirm the Δ curl index measurements. Results of this study suggest there is a preferential energy absorption by the earlywood in the fiber aggregates compressed at low frequencies and with the initial compression cycle.

INTRODUCTION

Tree with both earlywood and latewood within the annual growth ring have inherent variation in local mechanical properties because of the presence of these different fiber types. Earlywood fibers are generally shorter, thinner-walled, and larger diameter with a higher fibril angle compared

to latewood fibers.[1] In wood, the strength, work to maximum load, elongation and modulus of elasticity differ greatly between the two growth regions, with earlywood having the smaller values.[2-7] Tensile testing of microspecimens showed a difference in the mode of fracture of the specimens. Earlywood had a tendency to break across the cell walls while latewood fibers failed between cells, in the middle lamella. Single fiber testing shows that the strength of the latewood tracheid is superior.[7]

In the southern pines, earlywood and latewood fibers have a marked difference in anatomical dimensions. Compared to the northern softwoods, the southern pines have a much larger proportion of latewood in the annual ring. The latewood fibers have an average wall thickness approximately double the earlywood fibers. A histogram comparing the wall thickness of the two fiber types, shows a bimodal distribution (Fig. 1). Tracheid diameter is larger for earlywood, due to a larger lumen. The larger diameter with less cell wall material leads to a lower specific gravity for the earlywood. Latewood fibers are also slightly longer than earlywood fibers at all heights and ages.[1]

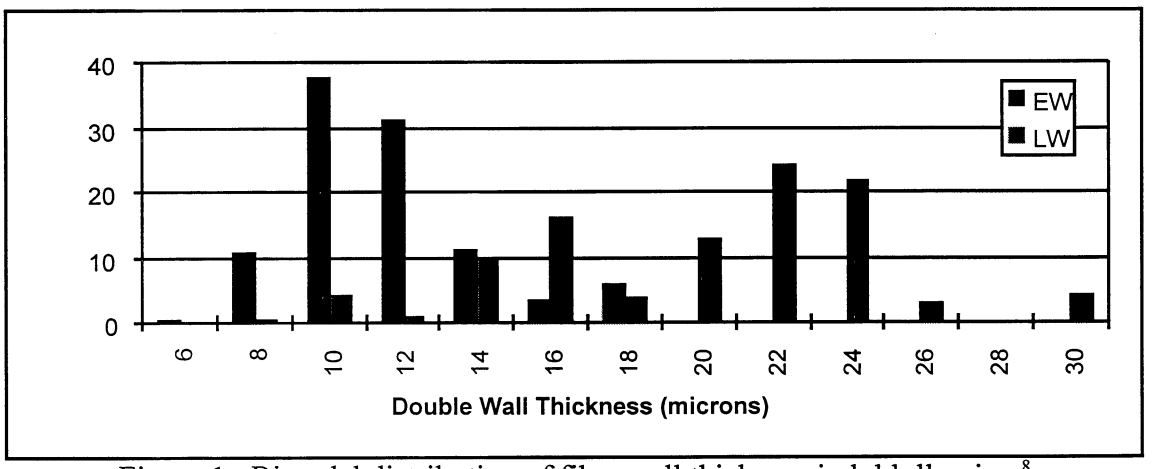

Figure 1. Bimodal distribution of fiber wall thickness in loblolly pine.[8]

Fiber defects, such as kinks and curl, lower the elastic modulus of the fiber and its capability to transmit stress along the fiber length.[9] Fibril angle, size and distribution of pits, degree of crystallinity and composition of the cell wall also influence fiber strength.[10]

TESTING METHODS

Wood Blocks

Studies of wood fatigue under conditions that simulate the cyclic compression of a refiner started with Salmén, Fellers, and Tigerström.[11-14] These researchers were trying to understand why the calculations of the energy required for fiber separation and flexiblization fell short of actual industry averages of energy required to achieve these processes in a refiner. Dumbbell- shaped pieces of wood were tested at various frequencies, temperatures, amplitudes, and grain direction.

They concluded that much of the energy in refining was consumed in viscoelastic energy absorption by the wood. They found that greater fatigue occurred with lower frequency, higher amplitude, and higher temperature.

Later work by Hickey and Rudie also focused on cyclic compression of wood blocks, but concentrated on differences in the earlywood and latewood sections of the wood.[15] The blocks were videotaped during the compression sequence and the width of the zones of earlywood and latewood measured before compression and then at predetermined compressions. Miniature thermocouples (0.5 mm) also were inserted in the dumbbell body and in the earlywood and latewood sections within the necked down portion of the dumbbell.

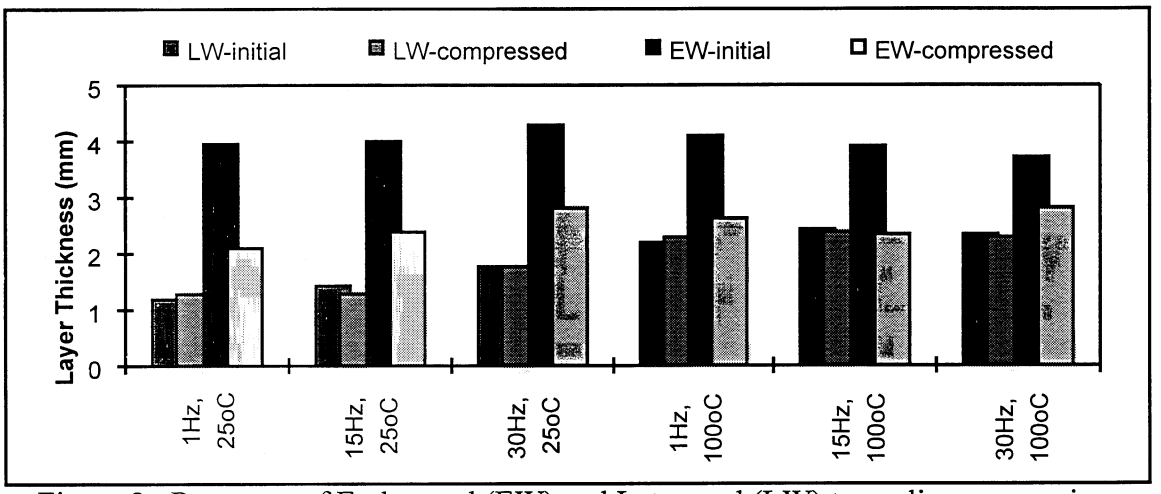

Figure 2. Response of Earlywood (EW) and Latewood (LW) to cyclic compression. Compressed width after 10,000 cycles.[15]

Figure 2 shows the thickness of the growth zones of the wood before the initial compression, and the compressed position after 10,000 compression cycles.[15] The earlywood portion is compressed to 63% of the initial width, but the latewood zone is only compressed to 97% of initial width. Temperature and frequency had little effect upon this response. The earlywood began absorbing energy and the temperature rose immediately as the compression sequence begins (Figure 3). The latewood temperature began to rise a short time later, but never reached the temperature level of the earlywood. This temperature difference at equilibrium and the time lag are dependent upon the latewood band width, indicating that the latewood heating may be due to the thermal conductivity of the wood (Fig. 4).[15]

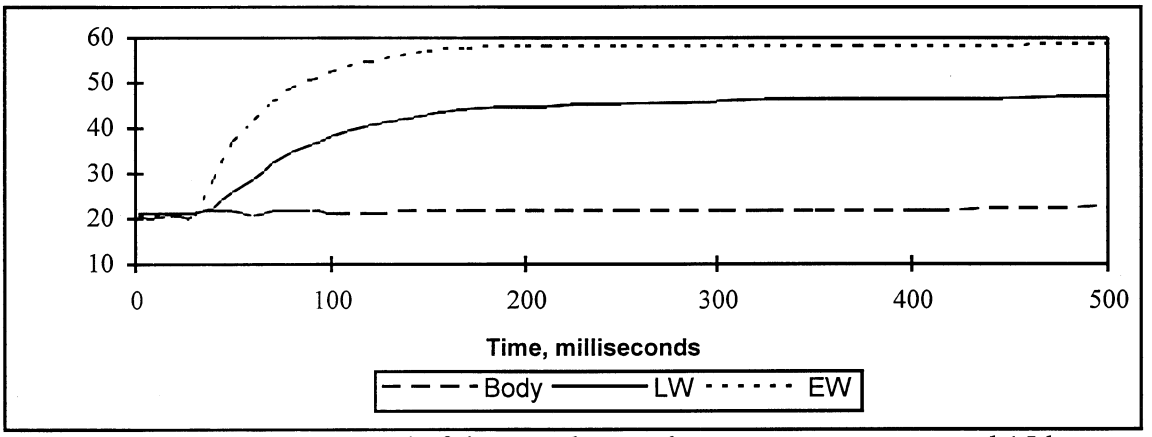

Figure 3. Temperature record of the sample tested at room temperature and 15 hertz. EW-LW-EW test piece.[15]

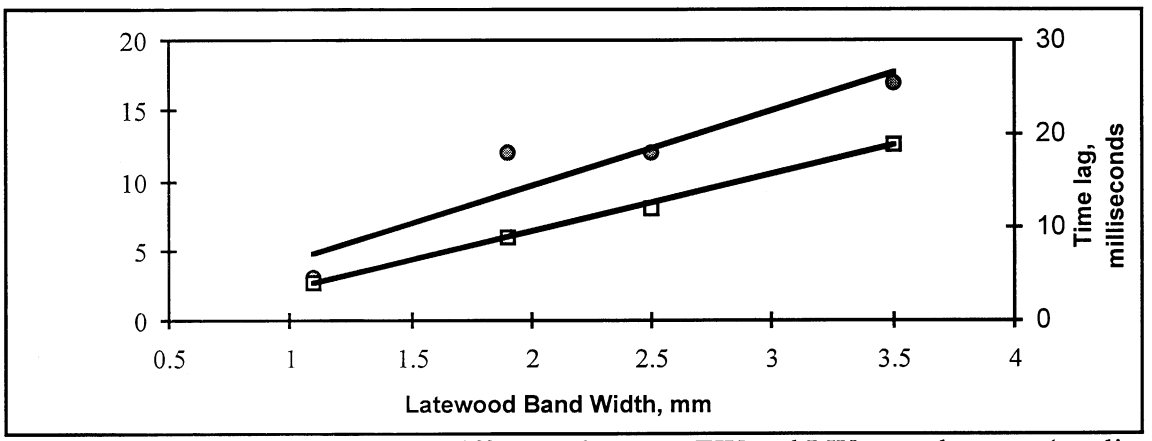

Figure 4. Equilibrium temperature difference between EW and LW growth zones (top line, R^2=0.88) and time delay for the latewood band to rise 50° C (bottom line, R^2=0.99).[15]

Wood Particles

If preferential energy absorption is occurring, then earlywood should break up earlier in the refining process, and the earlywood should be concentrated in the smaller size fractions of the pulp. To test this theory, wood chips were refined at low energy input (20kW-h/t) in an Asplund Defibrator D.[16] After refining, the chips were fractionated on a Bauer-McNett apparatus with 4-, 8-, 20-, and 100-mesh wire screens. The pulps captured by each screen were delignified using acidic sodium chlorite. The coarseness of each fraction was measured and compared to chlorite-pulped samples of pure earlywood and latewood fibers. The 4- and 8-mesh samples have coarseness values close to that of a whole pulp, while the 20- and 100-mesh samples have a value close to pure earlywood (Table 1). This shows a slight enrichment of the small size fractions with earlywood as expected.

Table 1. Coarseness and fiber lengths for the various samples.[8]

Sample of Mesh	Coarseness (mg/m)	Fiber Length (mm)
EW	0.16	2.80
LW	0.38	3.26
4	0.22	3.21
8	0.21	2.94
20	0.17	2.62
100	0.18	1.21

Cyclic Compression and Preferential Energy Absorption in Fiber Aggregates

Experimental. A loblolly pine (*Pinus teada*) log was cut into approximately one inch discs, and the discs cut into wedges. The wedges were then chipped with a modified hand press fitted with a chisel blade. Wood from the 15th to the 35th annual rings was used in these experiments. Wood in each of the annual rings was separated into earlywood, transitional wood, and latewood using the hand press. Earlywood and latewood chips were refined separately at low energy input in an Asplund Defibrator D. Pulps were fractionated in a Bauer-McNett fiber classifier with 4-, 14-, 28-, and 48-mesh screens. The separated and fractionated pulps were bagged, flushed with nitrogen gas, sealed, and pasteurized.[17,18] The bags were then placed into a cold room for storage.

The fiber aggregate sample size was determined by stopping a 12" Sprout Waldron refiner while under load. The refiner was opened and six fiber bundles extracted and measured for volume. They were then oven dried and weighed. This gave a density and, knowing the volume within the cuvet, a fiber mass was calculated.

The fibers in the aggregate are mixed in a 50/50 ratio by mass of earlywood and latewood, using fibers from the retained 28-mesh screen. For the video imaging, 5% of either the earlywood or latewood is stained with a fluorescent dye. The fibers are mixed and brought to a 30% consistency. For the thermal imaging, either all the earlywood or latewood is stained with the same dye, mixed, and then brought to 45 % consistency (a higher consistency is needed due to the blocking effect of water to infrared energy).

The initial experimentation has been completed using 10 and 30 hertz frequency, with a peak-to-peak amplitude of one millimeter on a MTS(the MTS was controlled for stroke distance). The video images were analyzed using an Optimas image analysis system. The curl index[19-20] for each stained fiber in the microscope view is determined before starting and after 1, 10, 100, 1000, 10,000 cycles and each half cycle following the indicated cycle.

The majority of the infrared imaging has been completed with analysis of the images currently in progress. This part of the study was done at Oak Ridge National Laboratory in Oak Ridge Tennessee using their Amber Galileo thermal imaging equipment and a 4X infrared lens (co-purchased with IPST). This used the shaker assembly built at IPST to compress the aggregates.

Discussion. The average values of curl index at 10 hertz are shown in Fig. 5. In this figure, the filled square symbols show the average curl index of the earlywood fibers after complete cycle, which can be compared to the open squares of the earlywood fibers after half of a cycle. The filled and empty circle symbols show the same data for the latewood fibers. This raw data does not seem to support the idea of preferential energy absorption by the earlywood fibers. When the absolute value of the difference in curl index data from matched fibers at both complete and half compression state is averaged, it becomes apparent that the earlywood fibers absorb the compression, and there is relatively little change in shape for the latewood fibers within a compression cycle (Fig. 6). The earlywood fibers are moving and flexing more than the latewood fibers. The average absolute value of change in curl index within a cycle is significantly different after 10, 100, and 1000 compression cycles (Appendix). The 30 hertz data also shows slightly more flexing within cycles for the earlywood fibers than the latewood fibers, significant at about 90% using a t-test (Appendix).

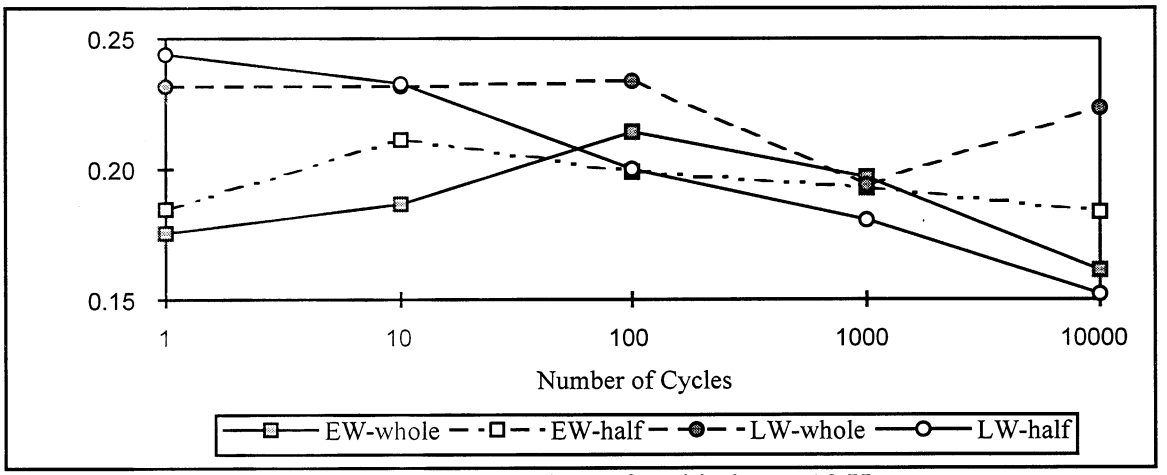

Figure 5. Average values of curl index at 10 Hz.

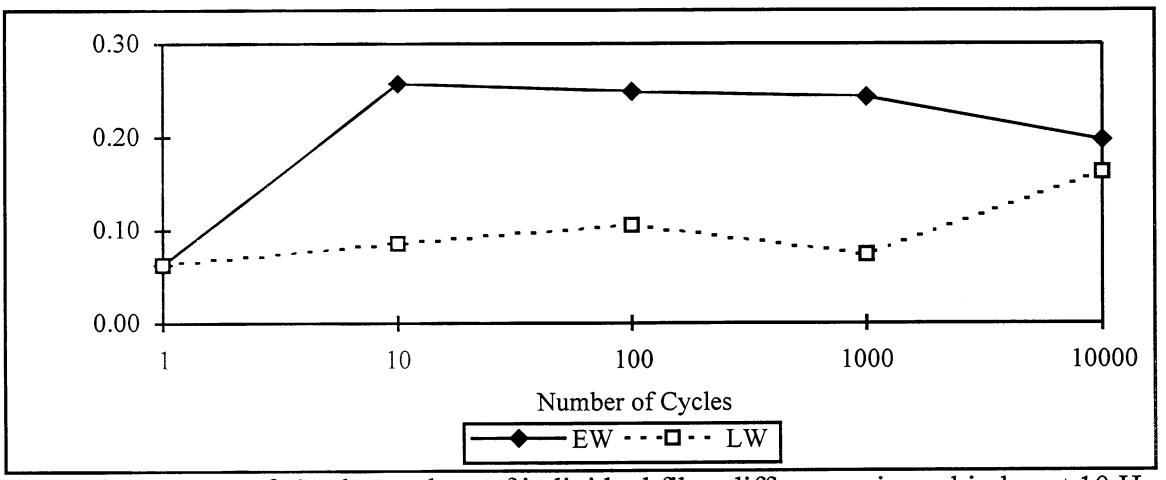

Figure 6. Average of absolute values of individual fiber differences in curl index at 10 Hz.

The average change in temperature at 10 hertz is shown in Figure 7. This shows a general decrease in average fiber temperature compared to the temperature prior to cycling and that both fiber types behave similarly. These decreasing temperatures are probably due to air being pumped in and out of the cell holding the fiber aggregate by the motion of the piston. The temperature

decrease holds relatively steady for the first 1000 compressions and then plummets. It is theorized that the fiber aggregate no longer expands after about 1000 compression, and therefore energy is no longer being absorbed by the fibers. Of interesting is that the temperature rises in the first compression and that the earlywood fibers show a significantly higher temperature increase compared to the latewood fibers. It appears that preferential energy absorption occurs in the initial compression at this frequency (Appendix). The first compression is of special interest because in a refiner, fiber aggregates are continuously being rolled, shredded and reformed and any particular aggregate is probably staying together for only one compression pulse. The Appendix also contains the graphs for 30 and 50 hertz testing , and the respective t-tests for significant differences between earlywood and latewood curl and temperature.

10 Hertz

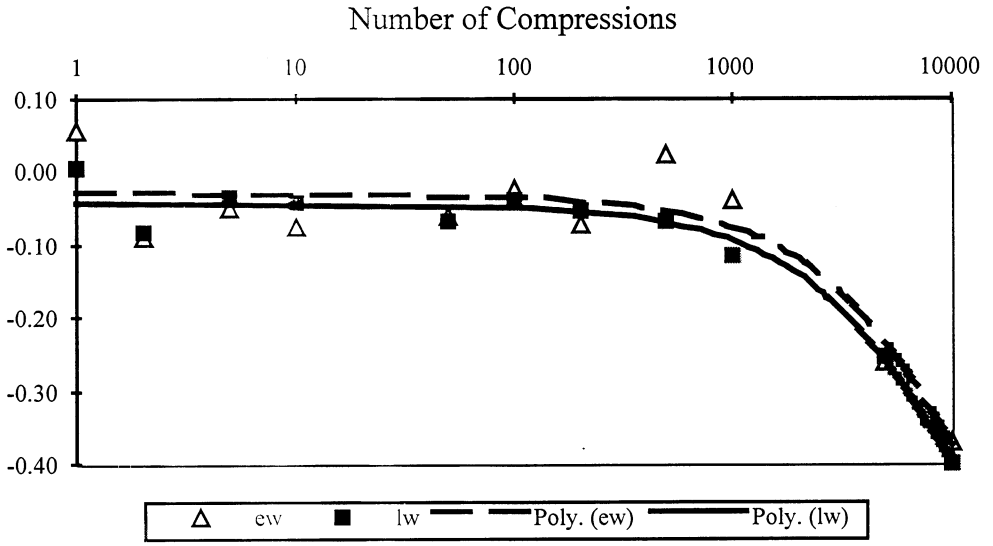

Figure 7. Change in average fiber temperature at 10 hertz.

CONCLUSION

Earlywood and latewood fiber aggregates appear to behave similarly in cyclic compression at low frequencies. While latewood has a high change in mean curl index relative to the initial uncompressed state, the change in curl index within a compression cycle is quite small. The earlywood fibers have a smaller change in curl index relative to the initial state, but show a greater change in curl index within each cycle. This within cycle flexing should increase the fatigue rate for the earlywood fibers. When the curl index data for 10 and 30 hertz are plotted on the same graph, it can be seen that at lower frequencies more energy is being absorbed per cycle in both earlywood and latewood. At higher frequencies, there is less energy absorbed in each cycle, and less preferential energy absorption by earlywood. This seems to show the same trend toward frequency that Salmen has seen.

The thermal imaging experiments also show energy absorption occuring if the cooling due to air flow is discounted. The initial compression is of interest due to its modeling of a true aggregate

behavior within the refiner. It shows that the most energy is applied in the first compression, with some preferentially absorption by the earlywood fiber. Therefore, even at the fiber aggregate stage there is still preferential energy absorption at very low frequencies. But, as frequency increases the difference may prove to be insignificant.

FUTURE WORK

The curl index studies will be done at higher frequencies using Dr. Aidun's high speed video equipment.

REFERENCES

1. Koch, P., *Utilization of the Southern Pines*, U.S. Department of Agriculture Forest Service, Vol. 1, p.83, (1972).

2. Kennedy, R.W., and Ifju, G., *Tappi Journal*, "Applications of Microtensile Testing to Thin Wood Sections," **45**(9):725(1962).

3. Kennedy, R.W., *Tappi Journal*, "Intra-increment Variation and Heritability of Specific Gravity, Parallel-to-Grain Tensile Strength, Stiffness, and Tracheid Length, in Clonal Norway Spruce," **49**(7):292(1966).

4. Ifju, G., *Wood Science*, "Within-Growth-Ring Variation in Some Physical Properties of Southern Pine Wood," **2**(1):11(1969).

5. Nordman, L.S., and Qvickstrom, B., *The Physics and Chemistry of Wood Pulp Fibers,* "Variability of the Mechanical Properties of Fibers Within a Growth Period," TAPPI Press, 1970, ed. D.H. Page, p. 177.

6. Biblis, E.J., *Wood Science and Technology*, "Transitional Variation and Relationships Among Properties Within Loblolly Pine Growth Rings," 3:14(1969).

7. Wellwood, R.W., *Pulp and Paper Magazine of Canada*, "Tensile Testing of Small Wood Samples," (2):T61(1962).

8. Rudie, A.W., Morra, J., St. Laurent, J., and Hickey, K.L., *Tappi Journal*, "The Influence of Wood and Fiber Properties on Mechanical Pulping,"77(6):86(1994).

9. Page, D.H., El-Hosseiny, F., Winkler, K., and Lancaster, A.P.S., *Tappi Journal*, "Elastic Modulus of Single Wood Pulp Fibers," **60**(4):114(1977).

10. Schniewind, A.P., *Proceedings of the Conference on the Mechanical Behavior of Wood*, "Mechanical Behavior of Wood in the Light of Its Anatomic Structure," p. 136(1962).

11. Salmen, N.L., and Fellers, C., *Transactions, Technical Section CPPA*, "The Fundamentals of energy Consumption During Viscoelastic and Plastic Deformation of Wood," **8**(4):TR93(1982).

12. Salmen, N.L., Fellers, C., Tigerstrom, A., *1983 International Mechanical Pulping Proceedings*, "The Effect of Loading Mode on the Energy Consumption during Mechanical Treatment of Wood," p.109.

13. Salmen, A. Tingerstrom, A., and Fellers, C., *Journal of Pulp and Paper Science,* "Fatigue of Wood - Characterization of Mechanical Defibration," **11**(3):J68(1985).

14. Salmen, L., Chip Refining: Influence of Mechanical and Chemical Treatments on the Energy Consumption During Fatigue of Wood, STFI-meddelande serie A, NR 964, (1986), p.1.

15. Hickey, K.L., Rudie, A.W., *EUCEPA*, 18th International Mechanical Pulping Conference - Poster Presentation, Oslo, Norway, June 15-17, 1993, "Preferential Energy Absorption by Earlywood in Cyclic Compression of Loblolly Pine," p. 81.

16. St. Laurent, J.M., Rudie, A.W., and Shakhet, A.R., *Proceedings, 1993 TAPPI Pulping Conference*, "Mechanical Pulping by Fractionation After Low Energy Refining" Atlanta, Nov. 1-3, p.95.

17. Zabel, R.Z., and Morrell, J.J., *Wood Microbiology, Decay and its Prevention*, 1992, p. 101.

18. Panshin, A.J., and DeZeeuw, C., *Textbook of Wood Technology*, McGraw-Hill, 1980, p. 358.

19. Page, D.H., Seth, R.S., Jordan, B.D., and Barbe, M.C., *Papermaking Raw Materials*, "Curl, Crimps, Kinks and Microcompressions in Pulp Fibres - Their Origin, Measurement and Significance," Mechanical Engineering Publications, Ltd., ed. V. Punton, 1985, p. 183.

20. Jordan, B.L., and Nguyen, N.G., *Paperi ja Puu*, "Curvature, Kink and Curl," (4):313(1986).

APPENDIX t-test of averaged absolute value differences within cycles for individual fibers of earlywood and latewood.

t-Test: Two-Sample Assuming Unequal Variances , 10 Hz

Absolute(1-1.5)	*EW*	*LW*
Mean	0.064	0.056
Variance	0.005	0.006
Observations	46	52
Hypothesized Mean Difference	0	
df	96	
t Stat	0.548	
P(T<=t) one-tail	0.292	
t Critical one-tail	1.661	
P(T<=t) two-tail	0.585	
t Critical two-tail	1.985	

Absolute(10-10.5)	*EW*	*LW*
Mean	0.257	0.086
Variance	0.052	0.019
Observations	46	52
Hypothesized Mean Difference	0	
df	72	
t Stat	4.391	
P(T<=t) one-tail	0.000	
t Critical one-tail	1.666	
P(T<=t) two-tail	0.000	
t Critical two-tail	1.993	

Absolute(100-100.5)	*EW*	*LW*
Mean	0.248	0.105
Variance	0.062	0.062
Observations	46	52
Hypothesized Mean Difference	0	
df	95	
t Stat	2.839	
P(T<=t) one-tail	0.003	
t Critical one-tail	1.661	
P(T<=t) two-tail	0.006	
t Critical two-tail	1.985	

Absolute(1000-1000.5)	*EW*	*LW*
Mean	0.244	0.074
Variance	0.068	0.011
Observations	46	52
Hypothesized Mean Difference	0	
df	58	
t Stat	4.144	
P(T<=t) one-tail	0.000	
t Critical one-tail	1.672	
P(T<=t) two-tail	0.000	
t Critical two-tail	2.002	

Absolute(10,000-10,000.5)	*EW*	*LW*
Mean	0.196	0.163
Variance	0.043	0.037
Observations	46	52
Hypothesized Mean Difference	0	
df	92	
t Stat	0.808	
P(T<=t) one-tail	0.211	
t Critical one-tail	1.662	
P(T<=t) two-tail	0.421	
t Critical two-tail	1.986	

Figure 5. Average Absolute Curl Index at 10 Hertz, 5 to 4mm cycling and 30 Hertz, 4 to 3mm cycling.

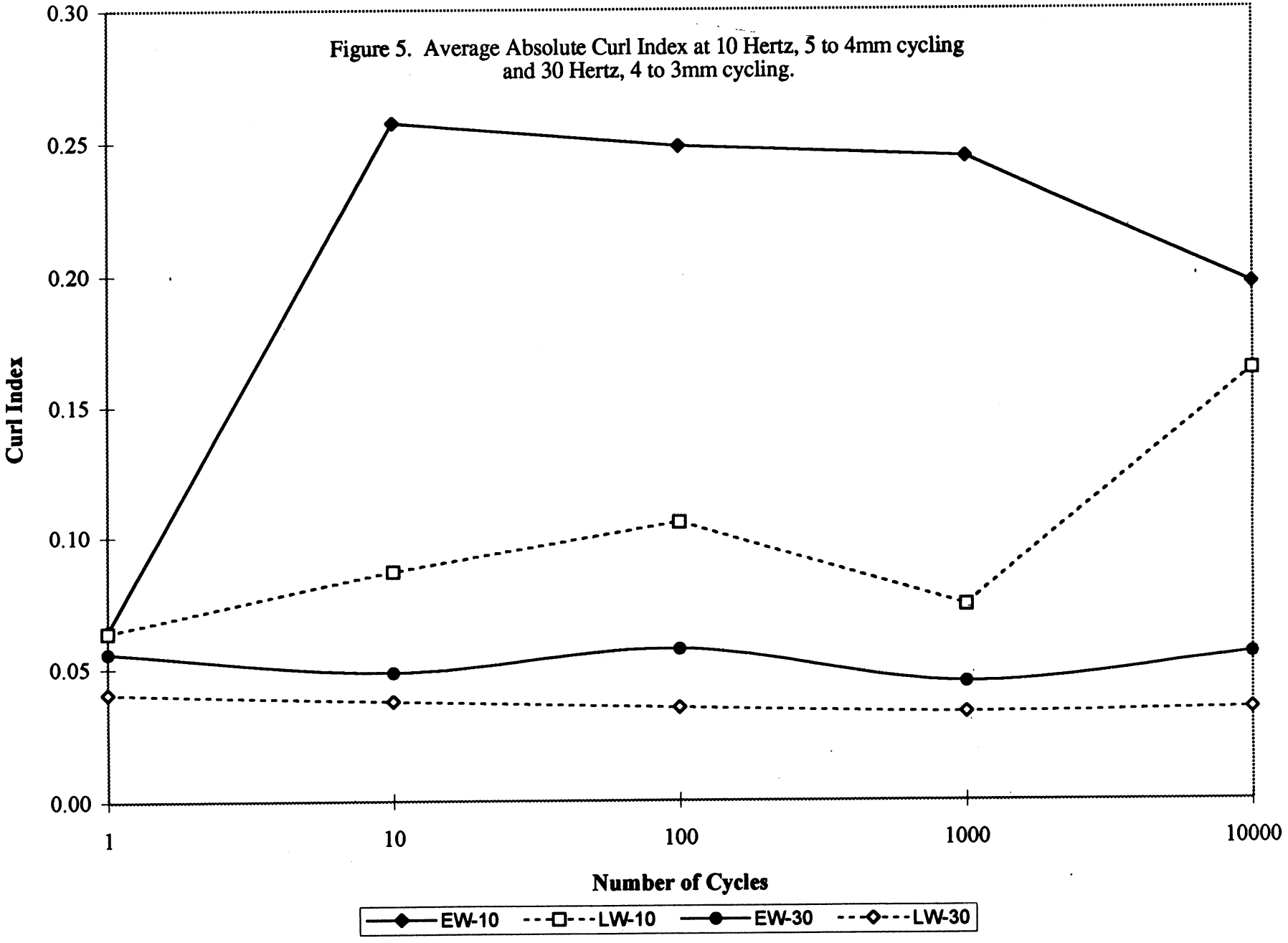

Table 2. t-test for average absolute curl index at 30 hertz, 4 to 3mm cycling.

t-Test: Two-Sample Assuming Unequal Variances			t-Test: Two-Sample Assuming Unequal Variances		
|1.5-1|	EW	LW	|10.5-10|	EW	LW
Mean	0.0340	0.0442	Mean	0.0280	0.0655
Variance	0.0006	0.0039	Variance	0.0010	0.0057
Observations	20	16	Observations	20	16
Hypothesized Mean Difference	0		Hypothesized Mean Difference	0	
df	19		df	19	
t Stat	-0.6142		t Stat	-1.8634	
P(T<=t) one-tail	0.2732		P(T<=t) one-tail	0.0390	
t Critical one-tail	1.7291		t Critical one-tail	1.7291	
P(T<=t) two-tail	0.5464		P(T<=t) two-tail	0.0779	
t Critical two-tail	2.0930		t Critical two-tail	2.0930	
t-Test: Two-Sample Assuming Unequal Variances			t-Test: Two-Sample Assuming Unequal Variances		
|100.5-100|	EW	LW	|1,000.5-1,000|	EW	LW
Mean	0.0339	0.0373	Mean	0.0227	0.0575
Variance	0.0021	0.0034	Variance	0.0004	0.0022
Observations	20	16	Observations	20	16
Hypothesized Mean Difference	0		Hypothesized Mean Difference	0	
df	28		df	19	
t Stat	-0.1894		t Stat	-2.7868	
P(T<=t) one-tail	0.4256		P(T<=t) one-tail	0.0059	
t Critical one-tail	1.7011		t Critical one-tail	1.7291	
P(T<=t) two-tail	0.8511		P(T<=t) two-tail	0.0118	
t Critical two-tail	2.0484		t Critical two-tail	2.0930	
t-Test: Two-Sample Assuming Unequal Variances					
|10,000.5-10,000|	EW	LW			
Mean	0.0340	0.0506			
Variance	0.0014	0.0036			
Observations	20	16			
Hypothesized Mean Difference	0				
df	24				
t Stat	-0.9699				
P(T<=t) one-tail	0.1709				
t Critical one-tail	1.7109				
P(T<=t) two-tail	0.3417				
t Critical two-tail	2.0639				

Thermal Analysis

t-Test: Two-Sample Assuming Unequal Variances			t-Test: Two-Sample Assuming Unequal Variances		
1	*LW*	*BW*	*200*	*LW*	*BW*
Mean	0.0061	0.0552	Mean	-0.0551	-0.0717
Variance	0.0051	0.0052	Variance	0.0162	0.0318
Observations	19	12	Observations	45	28
Hypothesized Mean Differenc	0		Hypothesized Mean Differenc	0	
df	23		df	44	
t Stat	-1.853		t Stat	0.429	
P(T<=t) one-tail	0.038		P(T<=t) one-tail	0.335	
t Critical one-tail	1.714		t Critical one-tail	1.680	
P(T<=t) two-tail	0.077		P(T<=t) two-tail	0.670	
t Critical two-tail	2.069		t Critical two-tail	2.015	
t-Test: Two-Sample Assuming Unequal Variances			t-Test: Two-Sample Assuming Unequal Variances		
2	*LW*	*BW*	*500*	*LW*	*BW*
Mean	-0.0821	-0.0907	Mean	-0.0677	0.0239
Variance	0.0119	0.0139	Variance	0.0193	0.0586
Observations	19	12	Observations	25	16
Hypothesized Mean Differenc	0		Hypothesized Mean Differenc	0	
df	22		df	21	
t Stat	0.204		t Stat	-1.375	
P(T<=t) one-tail	0.420		P(T<=t) one-tail	0.092	
t Critical one-tail	1.717		t Critical one-tail	1.721	
P(T<=t) two-tail	0.840		P(T<=t) two-tail	0.184	
t Critical two-tail	2.074		t Critical two-tail	2.080	
t-Test: Two-Sample Assuming Unequal Variances			t-Test: Two-Sample Assuming Unequal Variances		
5	*LW*	*BW*	*1000*	*LW*	*BW*
Mean	-0.0336	-0.0491	Mean	-0.1151	-0.0393
Variance	0.0052	0.0159	Variance	0.0160	0.0453
Observations	19	12	Observations	25	16
Hypothesized Mean Differenc	0		Hypothesized Mean Differenc	0	
df	16		df	22	
t Stat	0.388		t Stat	-1.286	
P(T<=t) one-tail	0.352		P(T<=t) one-tail	0.106	
t Critical one-tail	1.746		t Critical one-tail	1.717	
P(T<=t) two-tail	0.703		P(T<=t) two-tail	0.212	
t Critical two-tail	2.120		t Critical two-tail	2.074	
t-Test: Two-Sample Assuming Unequal Variances			t-Test: Two-Sample Assuming Unequal Variances		
10	*LW*	*BW*	*5000*	*LW*	*BW*
Mean	-0.0408	-0.0768	Mean	-0.2542	-0.2612
Variance	0.0137	0.0169	Variance	0.0240	0.0451
Observations	19	12	Observations	25	16
Hypothesized Mean Differenc	0		Hypothesized Mean Differenc	0	
df	22		df	25	
t Stat	0.778		t Stat	0.114	
P(T<=t) one-tail	0.222		P(T<=t) one-tail	0.455	
t Critical one-tail	1.717		t Critical one-tail	1.708	
P(T<=t) two-tail	0.445		P(T<=t) two-tail	0.910	
t Critical two-tail	2.074		t Critical two-tail	2.060	
t-Test: Two-Sample Assuming Unequal Variances			t-Test: Two-Sample Assuming Unequal Variances		
50	*LW*	*BW*	*10,000*	*LW*	*BW*
Mean	-0.0676	-0.0594	Mean	-0.3990	-0.3711
Variance	0.0082	0.0157	Variance	0.0375	0.0446
Observations	19	12	Observations	25	16
Hypothesized Mean Differenc	0		Hypothesized Mean Differenc	0	
df	18		df	30	
t Stat	-0.195		t Stat	-0.4274	
P(T<=t) one-tail	0.424		P(T<=t) one-tail	0.3361	
t Critical one-tail	1.734		t Critical one-tail	1.6973	
P(T<=t) two-tail	0.847		P(T<=t) two-tail	0.6721	
t Critical two-tail	2.101		t Critical two-tail	2.0423	
t-Test: Two-Sample Assuming Unequal Variances					
100	*Variable 1*	*Variable 2*			
Mean	-0.0399	-0.0257			
Variance	0.0145	0.0296			
Observations	45	28			
Hypothesized Mean Differenc	0				
df	43				
t Stat	-0.382				
P(T<=t) one-tail	0.352				
t Critical one-tail	1.681				
P(T<=t) two-tail	0.705				
t Critical two-tail	2.017				

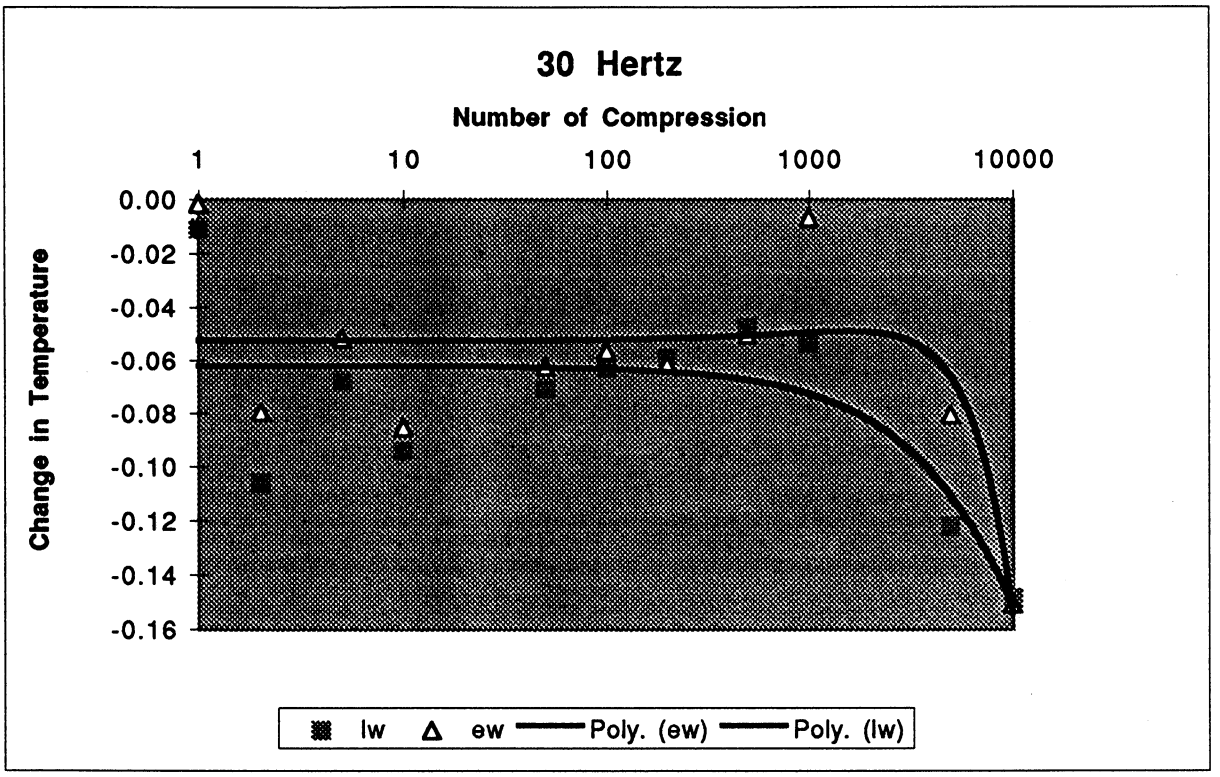
30 Hertz
Number of Compression
1
10
100
1000
10000
0.00
-0.02
-0.04
-0.06
-0.08
-0.10
-0.12
-0.14
-0.16
Change in Temperature
lw
ew
Poly. (ew)
Poly. (lw)

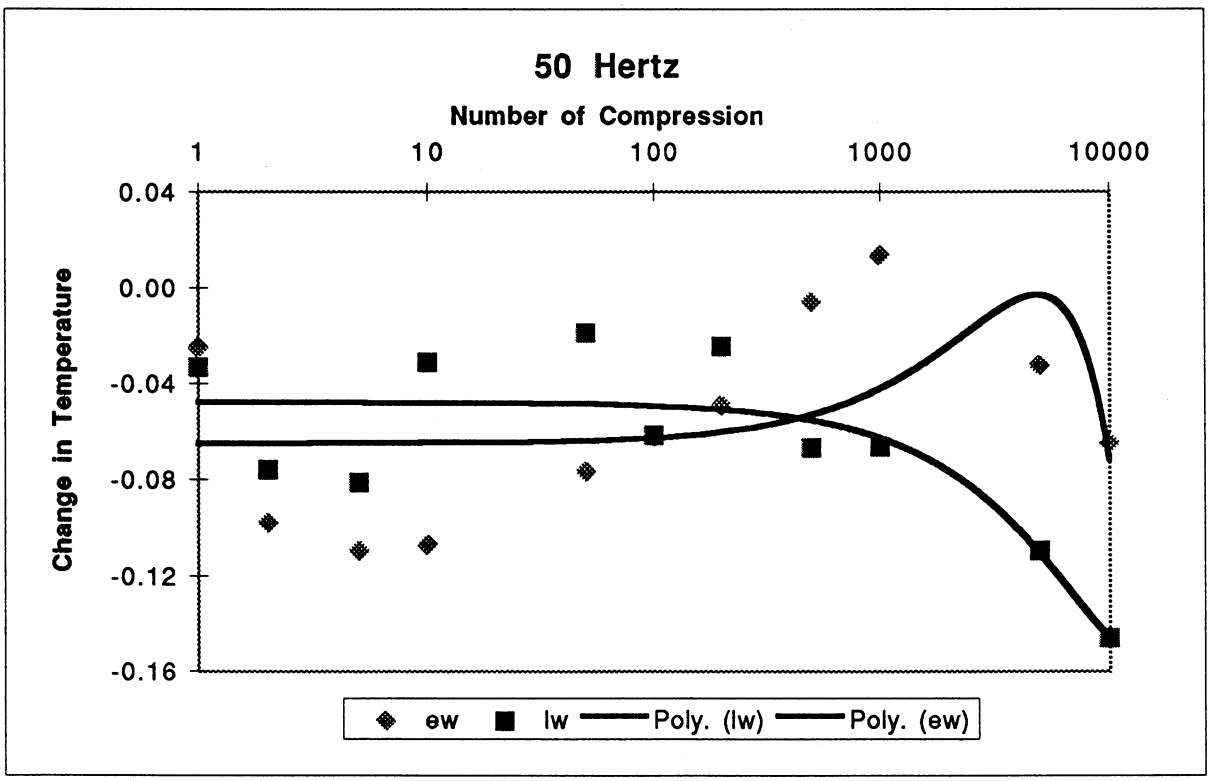
50 Hertz
Number of Compression
1
10
100
1000
10000
0.04
0.00
-0.04
-0.08
-0.12
-0.16
Change in Temperature
ew
lw
Poly. (lw)
Poly. (ew)

Thermal Analysis

t-Test: Two-Sample Assuming Unequal Variances			t-Test: Two-Sample Assuming Unequal Variances		
1	*LW*	*BW*	*200*	*LW*	*BW*
Mean	-0.0107	-0.0017	Mean	-0.0588	-0.0616
Variance	0.0098	0.0022	Variance	0.0163	0.0251
Observations	14	9	Observations	40	34
Hypothesized Mean Differen	0		Hypothesized Mean Differen	0	
df	20		df	63	
t Stat	-0.294		t Stat	0.084	
P(T<=t) one-tail	0.386		P(T<=t) one-tail	0.467	
t Critical one-tail	1.725		t Critical one-tail	1.669	
P(T<=t) two-tail	0.771		P(T<=t) two-tail	0.933	
t Critical two-tail	2.086		t Critical two-tail	1.998	
t-Test: Two-Sample Assuming Unequal Variances			t-Test: Two-Sample Assuming Unequal Variances		
2	*LW*	*BW*	*500*	*LW*	*BW*
Mean	-0.1059	-0.0797	Mean	-0.0477	-0.0502
Variance	0.0108	0.0208	Variance	0.0229	0.0308
Observations	14	9	Observations	26	25
Hypothesized Mean Differen	0		Hypothesized Mean Differen	0	
df	13		df	47	
t Stat	-0.474		t Stat	0.055	
P(T<=t) one-tail	0.322		P(T<=t) one-tail	0.478	
t Critical one-tail	1.771		t Critical one-tail	1.678	
P(T<=t) two-tail	0.644		P(T<=t) two-tail	0.956	
t Critical two-tail	2.160		t Critical two-tail	2.012	
t-Test: Two-Sample Assuming Unequal Variances			t-Test: Two-Sample Assuming Unequal Variances		
5	*LW*	*BW*	*1000*	*LW*	*BW*
Mean	-0.0679	-0.0517	Mean	-0.0531	-0.0066
Variance	0.0088	0.0148	Variance	0.0231	0.0314
Observations	14	9	Observations	26	25
Hypothesized Mean Differen	0		Hypothesized Mean Differen	0	
df	14		df	47	
t Stat	-0.340		t Stat	-1.005	
P(T<=t) one-tail	0.370		P(T<=t) one-tail	0.160	
t Critical one-tail	1.761		t Critical one-tail	1.678	
P(T<=t) two-tail	0.739		P(T<=t) two-tail	0.320	
t Critical two-tail	2.145		t Critical two-tail	2.012	
t-Test: Two-Sample Assuming Unequal Variances			t-Test: Two-Sample Assuming Unequal Variances		
10	*LW*	*BW*	*5000*	*LW*	*BW*
Mean	-0.0940	-0.0853	Mean	-0.1217	-0.0806
Variance	0.0130	0.0176	Variance	0.0341	0.0293
Observations	14	9	Observations	26	25
Hypothesized Mean Differen	0		Hypothesized Mean Differen	0	
df	15		df	49	
t Stat	-0.161		t Stat	-0.826	
P(T<=t) one-tail	0.437		P(T<=t) one-tail	0.206	
t Critical one-tail	1.753		t Critical one-tail	1.677	
P(T<=t) two-tail	0.874		P(T<=t) two-tail	0.413	
t Critical two-tail	2.131		t Critical two-tail	2.010	
t-Test: Two-Sample Assuming Unequal Variances			t-Test: Two-Sample Assuming Unequal Variances		
50	*LW*	*BW*	*10,000*	*LW*	*BW*
Mean	-0.0708	-0.0624	Mean	-0.1485	-0.1507
Variance	0.0130	0.0162	Variance	0.0597	0.0447
Observations	13	9	Observations	23	22
Hypothesized Mean Differen	0		Hypothesized Mean Differen	0	
df	16		df	43	
t Stat	-0.159		t Stat	0.033	
P(T<=t) one-tail	0.438		P(T<=t) one-tail	0.487	
t Critical one-tail	1.746		t Critical one-tail	1.681	
P(T<=t) two-tail	0.876		P(T<=t) two-tail	0.974	
t Critical two-tail	2.120		t Critical two-tail	2.017	
t-Test: Two-Sample Assuming Unequal Variances					
100	*Variable 1*	*Variable 2*			
Mean	-0.0627	-0.0566			
Variance	0.0241	0.0264			
Observations	40	34			
Hypothesized Mean Differen	0				
df	69				
t Stat	-0.163				
P(T<=t) one-tail	0.435				
t Critical one-tail	1.667				
P(T<=t) two-tail	0.871				
t Critical two-tail	1.995				

Thermal Analysis

t-Test: Two-Sample Assuming Unequal Variances			t-Test: Two-Sample Assuming Unequal Variances		
1	*LW*	*BW*	*200*	*LW*	*BW*
Mean	-0.0333	-0.0252	Mean	-0.0246	-0.0491
Variance	0.0073	0.0115	Variance	0.0292	0.0197
Observations	10	13	Observations	27	29
Hypothesized Mean Differenc	0		Hypothesized Mean Differenc	0	
df	21		df	50	
t Stat	-0.202		t Stat	0.582	
P(T<=t) one-tail	0.421		P(T<=t) one-tail	0.282	
t Critical one-tail	1.721		t Critical one-tail	1.676	
P(T<=t) two-tail	0.842		P(T<=t) two-tail	0.563	
t Critical two-tail	2.080		t Critical two-tail	2.009	
t-Test: Two-Sample Assuming Unequal Variances			t-Test: Two-Sample Assuming Unequal Variances		
2	*LW*	*BW*	*500*	*LW*	*BW*
Mean	-0.0759	-0.0981	Mean	-0.0668	-0.0058
Variance	0.0288	0.0273	Variance	0.0292	0.0170
Observations	10	13	Observations	17	16
Hypothesized Mean Differenc	0		Hypothesized Mean Differenc	0	
df	19		df	30	
t Stat	0.314		t Stat	-1.156	
P(T<=t) one-tail	0.378		P(T<=t) one-tail	0.128	
t Critical one-tail	1.729		t Critical one-tail	1.697	
P(T<=t) two-tail	0.757		P(T<=t) two-tail	0.257	
t Critical two-tail	2.093		t Critical two-tail	2.042	
t-Test: Two-Sample Assuming Unequal Variances			t-Test: Two-Sample Assuming Unequal Variances		
5	*LW*	*BW*	*1000*	*LW*	*BW*
Mean	-0.0814	-0.1098	Mean	-0.0664	0.0138
Variance	0.0243	0.0140	Variance	0.0331	0.0172
Observations	10	13	Observations	17	16
Hypothesized Mean Differenc	0		Hypothesized Mean Differenc	0	
df	16		df	29	
t Stat	0.479		t Stat	-1.458	
P(T<=t) one-tail	0.319		P(T<=t) one-tail	0.078	
t Critical one-tail	1.746		t Critical one-tail	1.699	
P(T<=t) two-tail	0.638		P(T<=t) two-tail	0.156	
t Critical two-tail	2.120		t Critical two-tail	2.045	
t-Test: Two-Sample Assuming Unequal Variances			t-Test: Two-Sample Assuming Unequal Variances		
10	*LW*	*BW*	*5000*	*LW*	*BW*
Mean	-0.0312	-0.1072	Mean	-0.1098	-0.0325
Variance	0.0180	0.0140	Variance	0.0231	0.0138
Observations	10	13	Observations	17	16
Hypothesized Mean Differenc	0		Hypothesized Mean Differenc	0	
df	18		df	30	
t Stat	1.415		t Stat	-1.639	
P(T<=t) one-tail	0.087		P(T<=t) one-tail	0.056	
t Critical one-tail	1.734		t Critical one-tail	1.697	
P(T<=t) two-tail	0.174		P(T<=t) two-tail	0.112	
t Critical two-tail	2.101		t Critical two-tail	2.042	
t-Test: Two-Sample Assuming Unequal Variances			t-Test: Two-Sample Assuming Unequal Variances		
50	*LW*	*BW*		*LW*	*BW*
Mean	-0.0189	-0.0766	Mean	-0.1461	-0.0649
Variance	0.0185	0.0199	Variance	0.0360	0.0194
Observations	10	13	Observations	17	16
Hypothesized Mean Differenc	0		Hypothesized Mean Differenc	0	
df	20		df	29	
t Stat	0.994		t Stat	-1.407	
P(T<=t) one-tail	0.166		P(T<=t) one-tail	0.085	
t Critical one-tail	1.725		t Critical one-tail	1.699	
P(T<=t) two-tail	0.332		P(T<=t) two-tail	0.170	
t Critical two-tail	2.086		t Critical two-tail	2.045	
t-Test: Two-Sample Assuming Unequal Variances					
100	*LW*	*BW*			
Mean	-0.0616	-0.0622			
Variance	0.0238	0.0183			
Observations	27	29			
Hypothesized Mean Differenc	0				
df	52				
t Stat	0.015				
P(T<=t) one-tail	0.494				
t Critical one-tail	1.675				
P(T<=t) two-tail	0.988				
t Critical two-tail	2.007				